



**HAL**  
open science

## The *Arabidopsis condensin CAP-D* subunits arrange interphase chromatin

Celia Municio, Wojciech Antosz, Klaus Grasser, Etienne Kornobis, Michiel van Bel, Ignacio Eguinoa, Frederik Coppens, Andrea Bräutigam, Inna Lermontova, Astrid Bruckmann, et al.

► **To cite this version:**

Celia Municio, Wojciech Antosz, Klaus Grasser, Etienne Kornobis, Michiel van Bel, et al.. The *Arabidopsis condensin CAP-D* subunits arrange interphase chromatin. *New Phytologist*, 2021, 230 (3), pp.972 - 987. 10.1111/nph.17221 . pasteur-03693359

**HAL Id: pasteur-03693359**

**<https://pasteur.hal.science/pasteur-03693359>**

Submitted on 10 Jun 2022

**HAL** is a multi-disciplinary open access archive for the deposit and dissemination of scientific research documents, whether they are published or not. The documents may come from teaching and research institutions in France or abroad, or from public or private research centers.

L'archive ouverte pluridisciplinaire **HAL**, est destinée au dépôt et à la diffusion de documents scientifiques de niveau recherche, publiés ou non, émanant des établissements d'enseignement et de recherche français ou étrangers, des laboratoires publics ou privés.



Distributed under a Creative Commons Attribution 4.0 International License

# The Arabidopsis condensin CAP-D subunits arrange interphase chromatin

Celia Municio<sup>1</sup> , Wojciech Antosz<sup>2</sup> , Klaus D. Grasser<sup>2</sup> , Etienne Kornobis<sup>3,4</sup> , Michiel Van Bel<sup>5</sup> , Ignacio Eguinoa<sup>5</sup> , Frederik Coppens<sup>5</sup> , Andrea Bräutigam<sup>1</sup> , Inna Lermontova<sup>1,6</sup> , Astrid Bruckmann<sup>7</sup> , Katarzyna Zelkowska<sup>1</sup>, Andreas Houben<sup>1</sup>  and Veit Schubert<sup>1</sup> 

<sup>1</sup>Leibniz Institute of Plant Genetics and Crop Plant Research (IPK) Gatersleben, Corrensstraße 3, D-06466, Seeland, Germany; <sup>2</sup>Cell Biology and Plant Biochemistry, Biochemistry Center, University of Regensburg, Universitätsstraße 31, D-93053, Regensburg, Germany; <sup>3</sup>Plate-forme Technologique Biomics – Centre de Ressources et Recherches Technologiques (C2RT), Institut Pasteur, 75015 Paris, France; <sup>4</sup>Hub de Bioinformatique et Biostatistique -Département Biologie Computationnelle, Institut Pasteur, 75015 Paris, France; <sup>5</sup>VIB-Ugent Center for Plant Systems Biology, Technologiepark 71, 9052, Gent, Belgium; <sup>6</sup>Mendel Centre for Plant Genomics and Proteomics, CEITEC, Masaryk University, Brno CZ-62500, Czech Republic; <sup>7</sup>Department for Biochemistry I, Biochemistry Center, University of Regensburg, Universitätsstraße 31, D-93053, Regensburg, Germany. Open access funding enabled and organized by Projekt DEAL.

## Summary

Author for correspondence:  
Veit Schubert  
Email: [schubertv@ipk-gatersleben.de](mailto:schubertv@ipk-gatersleben.de)

Received: 24 September 2020  
Accepted: 11 January 2021

New Phytologist (2021) 230: 972–987  
doi: 10.1111/nph.17221

**Key words:** *Arabidopsis thaliana*, chromatin organization, chromosomes, condensin, interphase nuclei, SMC proteins.

- Condensins are best known for their role in shaping chromosomes. Other functions such as organizing interphase chromatin and transcriptional control have been reported in yeasts and animals, but little is known about their function in plants.
- To elucidate the specific composition of condensin complexes and the expression of CAP-D2 (condensin I) and CAP-D3 (condensin II), we performed biochemical analyses in Arabidopsis. The role of CAP-D3 in interphase chromatin organization and function was evaluated using cytogenetic and transcriptome analysis in *cap-d3* T-DNA insertion mutants.
- CAP-D2 and CAP-D3 are highly expressed in mitotically active tissues. *In silico* and pull-down experiments indicate that both CAP-D proteins interact with the other condensin I and II subunits. In *cap-d3* mutants, an association of heterochromatic sequences occurs, but the nuclear size and the general histone and DNA methylation patterns remain unchanged. Also, CAP-D3 influences the expression of genes affecting the response to water, chemicals, and stress.
- The expression and composition of the condensin complexes in Arabidopsis are similar to those in other higher eukaryotes. We propose a model for the CAP-D3 function during interphase in which CAP-D3 localizes in euchromatin loops to stiffen them and consequently separates centromeric regions and 45S rDNA repeats.

## Introduction

Structural maintenance of chromosomes (SMC) complexes are present in prokaryotes and eukaryotes (Cobbe & Heck, 2004). They are essential for chromatin organization and dynamics, gene regulation, and DNA repair. In eukaryotes, six conserved SMC subunits form the core of three different complexes: cohesin, condensin, and the SMC5/6 complex. Cohesin is involved in sister chromatid cohesion and interphase chromatin arrangement. Condensin is involved in mitotic and meiotic chromosome organization (van Ruiten & Rowland, 2018; Skibbens, 2019). The SMC5/SMC6 complex contributes mainly to DNA repair and replication (Jeppsson *et al.*, 2014). Animals have two condensin complexes, condensin I and II (Ono *et al.*, 2003). In yeasts only one condensin complex, analogous to animal condensin I, exists (Freeman *et al.*, 2000; Hirano, 2012a). Condensin I and II share a core formed by SMC2 and SMC4 and differ in the associated proteins, which in condensin I are CAP-H, CAP-D2, and CAP-

G, and in condensin II are CAP-H2, CAP-D3, and CAP-G2 (Ono *et al.*, 2003; Hirano, 2012a). This composition is conserved in higher eukaryotes, although in *Drosophila* the subunit CAP-G2 of condensin II has not been detected (Herzog *et al.*, 2013). As proposed for Arabidopsis (Fig. 1), plants apparently have condensin I and II (Schubert, 2009; Smith *et al.*, 2014).

Condensins have been widely studied in humans, animals, and yeast for their role in shaping chromosomes. Together with topoisomerase II, condensins form a scaffold within human somatic metaphase chromatids (Maeshima & Laemmli, 2003). Depletion of condensin I results in short fuzzy metaphase chromosomes, while depletion of condensin II results in long and curly chromosomes (Ono *et al.*, 2003; Green *et al.*, 2012). Besides aberrant chromosome morphologies, chromosomes lacking several condensin subunits show anaphase bridges and other segregation defects (Freeman *et al.*, 2000; Hudson *et al.*, 2003; Ono *et al.*, 2003, 2004; Hirota *et al.*, 2004; Savidou *et al.*, 2005; Gerlich *et al.*, 2006; Hartl *et al.*, 2008). Both complexes may

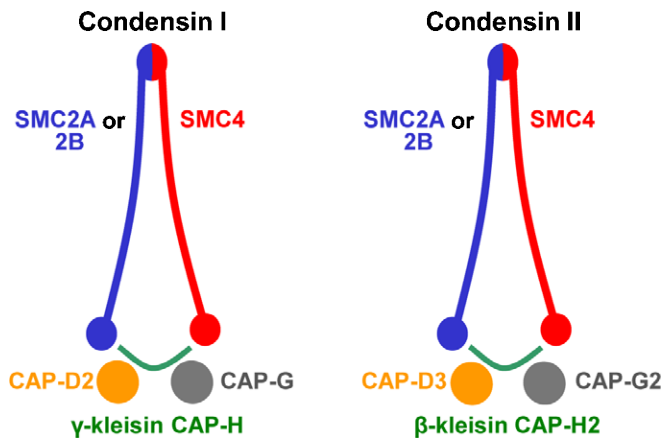


**Fig. 1** Arabidopsis condensin I and II subunit composition, based on the models of Nasmyth & Haering (2005) and Schubert (2009). Both condensin complexes can presumably be formed by SMC4 and two alternative SMC2 subunits (Siddiqui *et al.*, 2003). Condensin I contains (in addition to CAP-D2) CAP-G and the  $\gamma$ -kleisin CAP-H, and condensin II contains (in addition to CAP-D3) CAP-G2 and the  $\beta$ -kleisin CAP-H2 (www.arabidopsis.org; Fujimoto *et al.*, 2005). In the present work we confirm via analysis of CAP-D2 and CAP-D3 the interaction with the other respective subunits, and thus the presence of condensin I and II in Arabidopsis.

form DNA loops resulting in chromosome compaction (Gibcus *et al.*, 2018; van Ruiten & Rowland, 2018; Walther *et al.*, 2018; Elbatsh *et al.*, 2019).

In addition to the canonical role in metaphase chromosome formation, condensins are also involved in gene expression and chromatin organization during interphase (Wallace & Bosco, 2013; Wallace *et al.*, 2015). In mouse and human, condensin II localizes at the promoters of active genes and is required for normal gene expression (Downen *et al.*, 2013; Yuen *et al.*, 2017). In *Drosophila*, CAP-D3 together with the RetinoBlastoma protein RBF1 regulates gene clusters involved in tissue-specific functions (Longworth *et al.*, 2012), and condensin II promotes the formation of chromosome territories and keeps repetitive sequence clusters apart from each other (Hartl *et al.*, 2008; Bauer *et al.*, 2012; Hirano, 2012b; Rosin *et al.*, 2018).

In contrast to other organisms, Arabidopsis has two SMC2 homologs, SMC2A and SMC2B, with redundant functions (Siddiqui *et al.*, 2003) (Fig. 1). As in other species, SMC4, CAP-H, and CAP-H2 are present within chromosomes and are required for normal metaphase chromosome compaction (Fujimoto *et al.*, 2005; Smith *et al.*, 2014). CAP-D2 and CAP-D3 prevent the association of centromeres and induce chromatin compaction (Schubert *et al.*, 2013). The requirement of the condensin II-specific subunits CAP-H2 and CAP-G2 for keeping centromeres apart has been confirmed by Sakamoto *et al.* (2019). These authors also showed that condensin II is necessary for the correct spatial arrangement between centromeres and rDNA arrays.

Condensins are highly conserved but have not been studied extensively in plants. Here we analyze the Arabidopsis CAP-D2 and CAP-D3 condensin subunit expression patterns and interaction with other condensin subunits for a better understanding of their functions. We also demonstrate that Arabidopsis forms

specific condensin I and II complexes, and show that CAP-D3 mediates the spatial separation of chromocenters, without altering the global DNA or histone methylation patterns. Comparative transcriptome analyses revealed an influence of CAP-D3 on genes affecting the response to water, chemicals, and stress. Finally, we suggest a model explaining the action of CAP-D3 in preventing the association of chromocenters.

## Materials and Methods

### Plant material and stable transformation

All *Arabidopsis thaliana* (L.) Heynh lines and control plants are in the Columbia-0 (Col-0) background. The T-DNA *cap-d3* (SAIL\_826\_B06, SALK\_094776) insertion lines have previously been described in our laboratory (Schubert *et al.*, 2013). Seeds were sown in soil and germinated under short-day conditions (8 h : 16 h, light : dark; 18–20°C) and then transferred to long-day conditions (16 h : 8 h, light : dark; 18–20°C) before bolting. The lines were genotyped by polymerase chain reaction (PCR) using the primers listed in Supporting Information Table S1. The presence of the T-DNA was further confirmed by sequencing.

Stable Arabidopsis transformants were generated by the floral dip method (Clough & Bent, 1998). For the selection of primary transformants, the seeds were sterilized and plated on  $\frac{1}{2}$  Murashige & Skoog ( $\frac{1}{2}$ MS) basal medium (Sigma-Aldrich, St Louis, MO, USA) supplemented with the adequate antibiotics when required and grown in a growth chamber under long-day conditions.

### Transcript quantification

For transcript quantification total RNA was extracted from leaves of 6-wk-old and roots of 2-wk-old plants, complete 7-d-old seedlings, and flower buds of the whole inflorescence using the RNeasy Plant Mini kit (Qiagen, Venlo, the Netherlands) following the manufacturer's instructions. All RNA samples were treated with Turbo DNase (Thermo Fisher Scientific, Waltham, MA, USA) and tested for DNA contamination by PCR. Reverse transcription was performed using 250 ng of total RNA and the RevertAid H Minus First Strand cDNA Synthesis kit (Thermo Fisher Scientific), with oligo(dT)<sub>18</sub> primers, according to the manufacturer's instructions. The quality of the cDNA was checked with a PCR test targeting EF1B (Elongation factor 1 $\beta$ ) mRNA.

Real-time quantitative reverse transcription PCR (RT-qPCR) for *CAP-D2* and *CAP-D3* transcripts was performed in triplicate and from three independent biological samples using SYBR<sup>TM</sup> Green PCR Master Mix (Thermo Fisher Scientific) in a 7900HT Fast Real-Time PCR System (Applied Biosystems, Waltham, MA, USA). For each reaction, 0.5  $\mu$ l of cDNA template and 0.6 mM primers (Table S1) were used in 10  $\mu$ l. *PPA2* and *At4g26410* (Kudo *et al.*, 2016) were used as reference genes for data normalization, and the data were analyzed with the double delta Ct method (Livak & Schmittgen, 2001).

## CAP-D2 and CAP-D3 promoter::GUS reporter lines and $\beta$ -glucuronidase activity assay

Different lengths of the promoter regions of both *CAP-D2* and *CAP-D3* were cloned between the *SalI* and *NotI* restriction sites of the pEntr 1A plasmid (Invitrogen, Carlsbad, CA, USA). The sequences were amplified from gDNA with the primer pairs D2-1156F/D2ProR for the Pro1 fragment, D2-1156F/D2Int1R for Pro2, D2-1156F/D2Int2R for Pro3, D2-392F/D2ProR for Pro4, D2-392F/D2Int1R for Pro5, D2-392F/D2Int2R, for Pro6, D3-1318F/D3ProR for Pro7 and D3-474F/D3ProR for Pro8 (Table S1). The fragments were subcloned upstream of the GUS reporter gene in the pGWB633 plasmid (Nakamura *et al.*, 2010) using the Gateway LR Clonase II enzyme mix (Invitrogen) following the manufacturer's instructions.

Constructs were transformed into *Arabidopsis* and stable transformants were selected in  $\frac{1}{2}$  MS (Sigma-Aldrich) with  $16 \text{ mg l}^{-1}$  PPT (Duchefa, Biochemie BV, Haarlem, the Netherlands). One month after sowing, the plantlets were stained for GUS activity according to Jefferson *et al.* (1987) with small modifications. Plantlets were collected in 15 ml tubes containing 1% X-Glu (5-bromo-4-chloro-3-indolyl- $\beta$ -D-glucopyranoside; Duchefa) in 0.1 M phosphate buffer (pH 7.0). To facilitate the penetration of the solution into the material, the tubes containing the plant material and the staining solution were exposed to a vacuum for 5 min and incubated overnight at 37°C. The next day, the staining solution was replaced by 70% ethanol and incubated for 20 min at 60°C. This step was repeated until the chlorophyll was removed. The stained material was preserved in 70% ethanol at 4°C and analyzed under a stereomicroscope.

## cap-d3 SALK line complementation construct

The 3942 bp-long cDNA sequence of *CAP-D3* was synthesized and cloned into the pEntr 1A (Invitrogen) plasmid by the DNA-Cloning-Service (Hamburg, Germany). Once in the pEntr 1A plasmid, the coding sequence was subcloned into the pGWB641 plasmid (Nakamura *et al.*, 2010) using Gateway cloning (Invitrogen). The generated expression cassette contained CAP-D3 fused to EYFP C-terminally (*CAP-D3-EYFP*) under the control of the cauliflower mosaic virus 35S promoter.

## Affinity purification and mass spectrometry (AP-MS) of GS-tagged CAP-D2 and CAP-D3 from PSB-D cells

The cDNA sequences of *CAP-D3* and *CAP-D2* were synthesized and cloned into the pCambia 2300 35S GS-Ct plasmid by the DNA-Cloning-Service (Hamburg, Germany) resulting in the constructs pCambia2300\_CAP-D2\_GS and pCambia2300\_CAP-D3\_GS.

The *Arabidopsis* ecotype 'Landsberg erecta' cell suspension (PSB-D) was transformed as described previously (Van Leene *et al.*, 2015). CAP-D2-GS and CAP-D3-GS were affinity-purified following the protocol described by Dürr *et al.* (2014).

For mass spectrometry, the eluted proteins were separated in a 10% polyacrylamide gel and digested with trypsin. Mass spectrometry and data analysis were performed according to the

methods described by Antosz *et al.* (2017). PROTEINSCAPE v.3.1.3 (Bruker Daltonics, Bremen, Germany) in connection with MASCOT v.2.5.1 (Matrix Science, Chicago, IL, USA) facilitated database searching of the National Center for Biotechnology Information (NCBI) nr database.

Three independent affinity purifications were performed. A MASCOT score of a minimum of 100 and the presence in at least two of the purifications were considered as criteria for reliable protein identification. The experimental background (contaminating proteins that co-purified with the unfused GS-tag) and nonspecific interactions (proteins that co-purified independently of the bait used) were subtracted. The list of nonspecific *Arabidopsis* proteins is based on 543 affinity purification experiments using 115 different baits (Van Leene *et al.*, 2015).

## Nuclei preparations

*Arabidopsis* nuclei from differentiated leaf cells were isolated and flow-sorted according to their ploidy level, as described by Weishart *et al.* (2016), in a BD Influx Cell Sorter (BD Bioscience, Heidelberg, Germany). The nuclei were sorted based on their DNA content in 2C, 4C, 8C and 16C ploidy fractions. Next, 12  $\mu\text{l}$  of 4C sorted nuclei and the same amount of sucrose buffer (10 mM Tris, 50 mM KCl, 2 mM MgCl $\cdot$ 6H $_2$ O, 5% sucrose, pH 8.0) were placed on a slide. The slides were directly used or stored at  $-20^\circ\text{C}$ .

*Arabidopsis* nuclei were embedded in acrylamide to preserve their 3D structure following the procedure described by Kikuchi *et al.*, (2005) with modifications. On a slide, 12  $\mu\text{l}$  of nuclei suspension were mixed with 6  $\mu\text{l}$  of active 15% acrylamide embedding medium (15% acrylamide/bisacrylamide (29 : 1), 15 mM PIPES, 80 mM KCl, 20 mM NaCl, 2 mM EDTA, 0.5 mM EGTA, 0.5 mM spermidine, 0.2 mM spermine, 1 mM DTT, 0.32 M sorbitol, 2% APS and 2% Na $_2$ SO $_3$ ). A coverslip was carefully placed on top of the acrylamide–nuclei mixture and left to polymerize for 30 min at room temperature. The coverslip was then removed, leaving a thin pad of nuclei embedded in acrylamide on the slide that was directly used for fluorescence *in situ* hybridization (FISH).

## Probe preparation and FISH

The probes were generated via the following methods: by PCR for the 180 bp centromeric repeat (pAL; Martinez-Zapater *et al.*, 1986), from a plasmid for the 5S rDNA probe (pCT4.2; Campbell *et al.*, 1992), and from a bacterial artificial chromosome (BAC) containing the 45S rDNA repeats (BAC T15P10). The BAC was obtained from the *Arabidopsis* Biological Resource Center (Ohio, USA). The probes were labeled with modified dUTPs conjugated with Texas Red (Invitrogen) or Alexa488 (Invitrogen) by nick-translation. The FISH was performed as previously described (Pecinka *et al.*, 2004).

## Indirect immunofluorescence labeling

Nuclei and chromosome preparations were washed in 1 $\times$ PBS and incubated for 30 min at 37°C in a moist chamber with 30  $\mu\text{l}$

blocking buffer (4% BSA, 0.1% Tween-20 in 1×PBS) to reduce nonspecific antibody binding. After three washes in 1×PBS, the slides were incubated with the primary antibodies against histone H3K27me3, H3K9me1, H3K9me2, H3K4me3, H3K9ac, H3K14ac, H3K18ac or H3K9+14+18+23+27ac, and diluted in antibody buffer (1% BSA, 0.1% Tween-20 in 1×PBS) overnight at 4°C. The next day, the slides were washed in 1×PBS again and incubated with the secondary antibodies (anti-rabbit Alexa488, anti-rabbit rhodamine, or anti-mouse Alexa488), in antibody buffer for 1 h at 37°C. After incubation, the preparations were washed in 1×PBS, dehydrated in an ethanol series (70%, 90% and 96% ethanol for 2 min each) and counterstained with 4',6-diamidino-2-phenylindole (DAPI) in antifade (Vectashield, Vector Laboratories, Burlingame, CA, USA). All primary and secondary antibodies and the dilutions used are listed in Table S2.

Immunolocalization of 5-methyl-cytosine requires an initial DNA denaturation of the specimen. Therefore, slides with sorted nuclei were denatured in 70% formamide in 2×SSC for 2 min at 70°C. The preparations were dehydrated in ice-cold 70% and 96% ethanol for 5 min each and air-dried. Subsequent blocking and antibody incubation were carried out as described for the histone antibodies.

### Microscopy and image analysis

Wide-field fluorescence microscopy was used to evaluate and image the nuclei preparations with an Olympus BX61 microscope (Olympus, Tokyo, Japan) and an ORCA-ER CCD camera (Hamamatsu, Japan). The number of centromeric pAL, 45S rDNA and 5rDNA FISH signals per nucleus was quantified under the microscope. The differences in 45S rDNA signals per nucleus were tested with the Kruskal–Wallis test and Dunn's method. The localization patterns of the histone modifications and 5-methyl-cytosine were analyzed in *c.* 100 nuclei.

To analyze the ultrastructure of chromatin beyond the classical Abbe/Raleigh limit at a lateral resolution of *c.* 120 nm (super-resolution, achieved with a 488 nm laser) spatial structured illumination microscopy (3D-SIM) was applied using a ×63/1.4 Oil Plan-Apochromat objective of an Elyra PS.1 microscope system and the software ZENBLACK (Carl Zeiss GmbH, Jena, Germany). Maximum intensity projections of whole nuclei were calculated via the ZENBLACK software (Weisshart *et al.*, 2016). 3D rendering based on SIM image stacks was done using the IMARIS v.8.0 (Bitplane AG, Zurich, Switzerland) software.

The nuclear and centromeric areas were quantified on 16-bit grayscale microscopic images using IMAGEJ v.1.50i (Schneider *et al.*, 2012). The images were taken from preparations of flow-sorted nuclei. Since this technique flattens the nuclei, they were considered as two-dimensional. All images were treated the same way after using the same acquisition parameters. The nuclear area, measured based on DAPI staining, was delimited as a region of interest (ROI) with the RenyiEntropy threshold; the background was not subtracted. For the centromeric area, measured based on the pAL signal, the background was subtracted with the option 'rolling ball' set at 25 pixels, and the ROI was delimited with the RenyiEntropy threshold. The area of each ROI was

automatically measured by the program. Statistical analyses were performed on the nuclear and centromeric areas using one-way ANOVA and Tukey's HSD.

### Southern blot analysis

A 5 µg quantity of genomic DNA from Arabidopsis leaves was digested with either *Hpa*II or *Msp*I (Thermo Fisher Scientific). The DNA was gel-separated and transferred onto a nylon membrane (Hybond XL, Amersham). The <sup>32</sup>P-labeled centromeric 180 bp repeat pAL was used for Southern hybridization, and the signals were detected using autoradiography. The Arabidopsis centromeric pAL probe was generated by PCR and <sup>32</sup>P-labeled according to the manufacturer's instructions (Deca-Label DNA labeling Kit; Thermo Fisher Scientific).

### RNA-seq and comparative *in silico* transcriptome analysis

*cap-d3 SAIL*, *cap-d3 SALK*, and control (Col-0) seeds were sown in soil and grown under short-day conditions. RNA was extracted with the RNeasy Plant Mini Kit (Qiagen) from 50 mg of pooled 4-wk-old plantlets cut above the root. For each of the three Arabidopsis genotypes five independent RNA extractions were performed, and the RNA integrity of the samples was measured in a 2100 Bioanalyzer (Agilent, Technologies, Santa Clara, CA, USA). The four RNA samples of each genotype with the highest RNA integrity number (RIN) were used for library preparation and RNA sequencing (NGS platform, IPK Gatersleben, Germany). The libraries were prepared with a TruSeq RNA Library Kit (Illumina, San Diego, CA, USA) unstranded and sequenced in a HiSeq2000 system (single 100 bp reads).

The quality of the RNA-seq reads was assessed with FASTQC v.0.11.4 (Babraham Bioinformatics, Cambridge, UK) and the adaptors were trimmed with TRIMMOMATIC v.0.32 (Bolger *et al.*, 2014). After a second quality check in FASTQC, the reads were aligned with GSNAP v.2016-05-25 (Wu & Nacu, 2010) against the Arabidopsis TAIR10 genome, and the gene counts were calculated with HTSEQ v.0.6.1 (Anders *et al.*, 2015). Differential expression analyses were performed using the DESEQ2 v.1.14.0 BIOCONDUCTOR package (Love *et al.*, 2014). Genes were considered to be differentially expressed (DEG) when they had a Benjamini-Hochberg adjusted *P* value ≤ 0.05 and a log<sub>2</sub>-fold change ≤ -1 or ≥ 1. These steps were performed through GALAXY ( Afgan *et al.*, 2018). Genes detected as differentially expressed for both *cap-d3* mutants were considered to be the genes associated with CAP-D3 defective proteins independent of the specific mutation. Gene enrichment was analyzed with AGRIGO v.1.2 (Du *et al.*, 2010). The analysis of the transcription factors present in *cap-d3* DEG was performed using the Arabidopsis Transcription Factor Database (AtTFDB) from the Arabidopsis Gene Regulatory Information Server (AGRIS; Yilmaz *et al.*, 2011).

### Gene and protein identification numbers

Sequence data from this study can be found at The Arabidopsis Information Resource (TAIR, [www.arabidopsis.org](http://www.arabidopsis.org)) or the

National Center for Biotechnology Information (NCBI, [www.ncbi.nlm.nih.gov](http://www.ncbi.nlm.nih.gov)) databases under the following gene identification numbers: *CAP-D2*, AT3G57060; *CAP-D3*, AT4G15890.

## Results

### *CAP-D2* and *CAP-D3* are highly expressed in meristematic tissues

We assessed the transcription of both genes, *CAP-D2* (At3g57060) and *CAP-D3* (At4g15890), in seedlings, mature rosette leaves, roots, and flower buds by RT-qPCR. The highest transcription of both genes was observed in flower buds and the lowest in seedlings (Fig. 2). This observed transcription pattern agrees with the predicted expression pattern for both genes (Fig. S1). As in the predicted expression, we observed a lower expression in seedlings than in rosette leaves before flowering.

The activity of the *CAP-D2* and *CAP-D3* promoters was evaluated in *Arabidopsis* transgenic lines expressing different versions of the promoters fused to the  $\beta$ -glucuronidase (GUS) reporter gene (Fig. 3a). The promoter regions of *CAP-D2* and *CAP-D3* contain two putative E2F binding sites (Schubert *et al.*, 2013). Besides, promoter-proximal introns can enhance the expression of a gene by a mechanism known as Intron-Mediated Enhancement (IME) (Rose *et al.*, 2008). The putative enhancing ability of *CAP-D2* and *CAP-D3* introns was analyzed *in silico* with the web tool IMETER (Parra *et al.*, 2011). The IMETER score is positively correlated to the enhancing ability of an intron. For *CAP-D2* the two first introns have positive IMETER scores of 12.13 and 2.36, respectively, and were included in the analysis. However, the IMETER scores of the first two *CAP-D3* introns were negative,

–13.20 and –5.88 respectively, and not considered in the analysis. In total six presumed promoters of different lengths were analysed for *CAP-D2* and two for *CAP-D3*.

T1 transgenic plants with the different versions of *CAP-D2* and *CAP-D3* promoters were stained for GUS analysis (Fig. 3b). For Pro1 only, no positive plants could be isolated. The *CAP-D2* promoter version Pro2 ( $n=7$ ) was active in stipules (small organs at the base of the leaves), leaf vascular tissue, and root tip meristems. Pro3 ( $n=6$ ) had weak activity in root tips. All Pro4 plants ( $n=21$ ) showed GUS-staining in leaf vascular tissue and root tips, and in 16 plants also in stipules. All Pro5 plants ( $n=23$ ) presented GUS activity in the apical meristem and root tips, and in 16 of them also in leaf vascular tissue. Pro6 plants ( $n=5$ ) showed activity in roots, and in 3 plants also (weakly) in the apical meristem. Therefore, all *CAP-D2* promoter versions were active in root tips, but the staining was stronger in the short promoter versions (Pro4, Pro5, and Pro6) than in the long ones (Pro2 and Pro3). Also, the *CAP-D2* short promoters showed activity in the apical meristem, and versions that included the second intron (Pro3 and Pro6) lost the staining in the leaf vascular tissue. *CAP-D3* Pro7 showed no activity, and for Pro8 ( $n=8$ ), the plants showed activity in the apical meristem and root tips. For both *CAP-D2* and *CAP-D3*, the expression can be driven more effectively by the short promoters.

Taken together, RT-qPCR and GUS activity staining demonstrated that *CAP-D2* and *CAP-D3* are highly expressed in meristematic tissues (root tip meristem, flower buds, apical meristem) and less expressed in mature leaves. However, in one of our previous studies, immunostaining with anti-*CAP-D3* antibodies showed the presence of *CAP-D3* in differentiated leaf cell nuclei (Schubert *et al.*, 2013). Thus, we assume that condensins are required not only during cell divisions but also during interphase in nuclei of differentiated cells. A similar situation was observed for the centromere-specific histone H3 variant CENH3, which is highly expressed only in meristematic tissues, but the protein is also present in the nuclei of differentiated leaves in relatively large quantities (Heckmann *et al.*, 2011; Lermontova *et al.*, 2011).

### *CAP-D2* and *CAP-D3* interact with the other condensin subunits in specific complexes

*CAP-D2* and *CAP-D3* are specific components of the condensin I and II complexes, respectively. The presence of *CAP-D2* and *CAP-D3* as well as the other condensin complex subunits in *Arabidopsis* has been confirmed (Smith *et al.*, 2014), but whether the complexes are formed by the same subunits as in nonplant species is unknown. To predict the composition of each complex we identified *in silico* putative interactors of *CAP-D2* (Fig. S2a,c) and *CAP-D3* (Fig. S2b,c) using the STRING program (<http://string-db.org/>; Szklarczyk *et al.*, 2019). At the high score of >0.90 the proteins SMC2A (At5g62410), SMC2B (At3G47460), and SMC4 (At5g48600) were identified in interaction networks of both *CAP-D2* and *CAP-D3*, while CAP-G (At5g37630) and CAP-H (At2g32590) were found to be interactors of *CAP-D2*, and CAP-G2 (At1g64960) and CAP-H2 (At3g16730) were found to be specific interactors of *CAP-D3*.

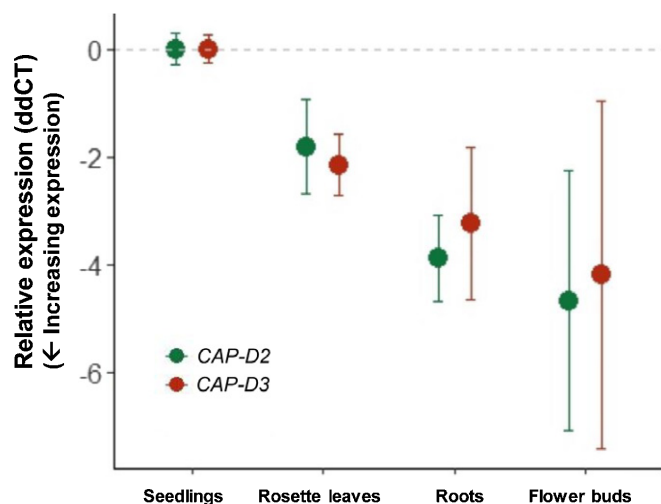


**Fig. 2** Transcript levels of *Arabidopsis* *CAP-D2* and *CAP-D3* in different tissues. Relative expression (ddCT) in flower buds, roots, and rosette leaves compared to seedlings. The values were normalized to the geometric mean of the housekeeping genes *PP2A* and *RHIP1* and relative to the expression in seedlings. The '0' does not indicate a lack of expression but that the expression in seedlings was used to calibrate the expression in the other tissues. Lower ddCT values indicate higher transcription. Error bars represent the SD between three biological replicates (each in triplicate).

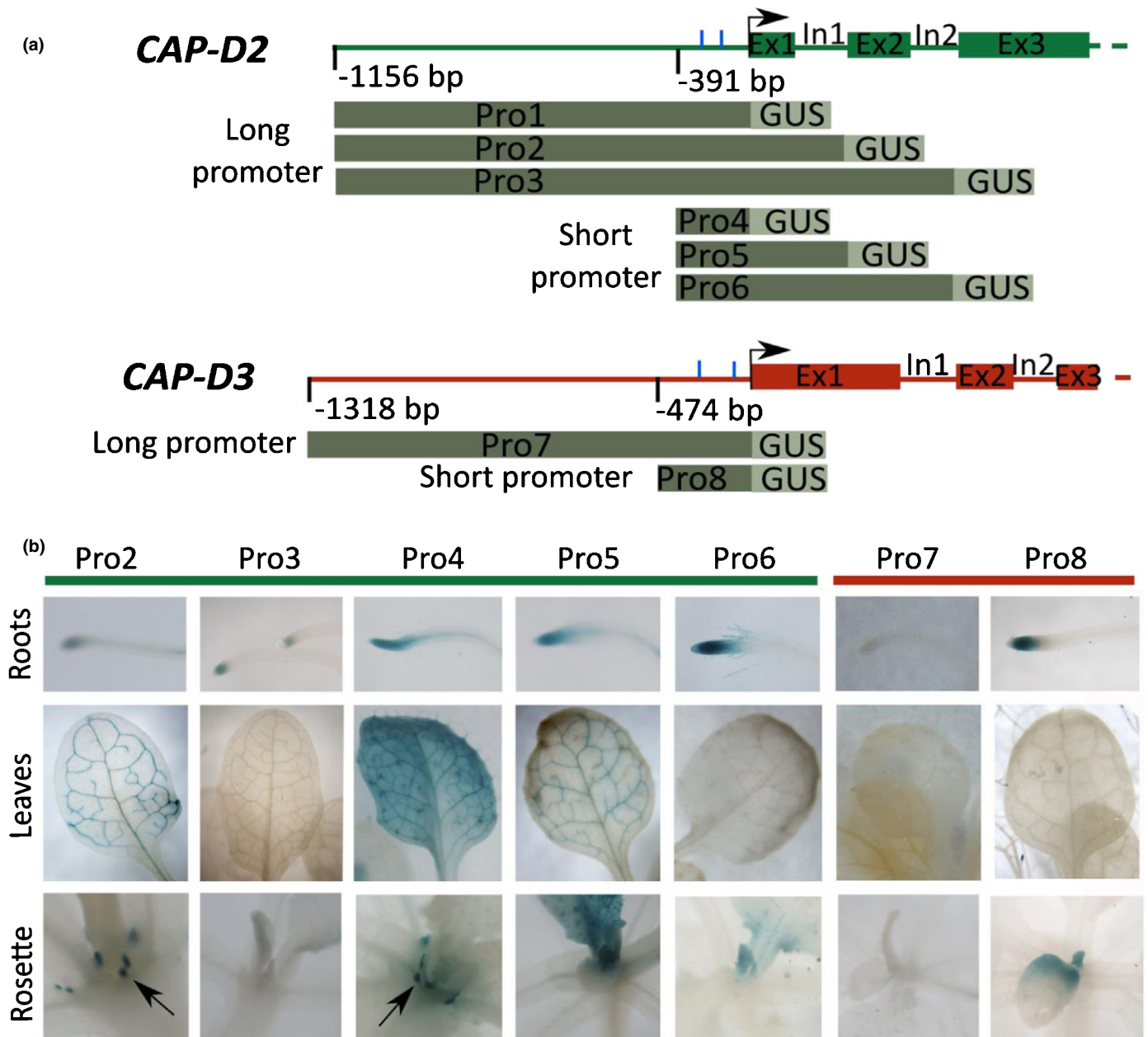


**Fig. 3** Arabidopsis *CAP-D2* and *CAP-D3* promoter activity. (a) Schematics depicting the promoter (Pro) regions, the first two introns (In) and three exons (Ex) of *CAP-D2* and *CAP-D3*. In each, the start of the coding region is marked by a black arrow, and the blue lines represent the position of the E2F binding sites. At the bottom of each schematic the different tested promoter versions fused to the GUS gene are represented. (b) Histochemical GUS staining (blue) in root meristems, leaves, stipules (arrows; Pro2, 4), and apical meristems of plants transformed with the indicated promoter versions Pro2-6 and Pro7-8. Images of Pro1 are not depicted since no transformants could be isolated.

Due to the presence of SMC2A, SMC2B, and SMC4 in both interaction networks, they may be involved in the formation of condensin I as well as condensin II. *In silico* analysis using the STRING program identified besides cohesin subunits also SMC5/6 complex subunits as *CAP-D2* and *CAP-D3* interacting partners (Zelkowski *et al.*, 2019).

To confirm these *in silico* predictions and to determine the composition of each complex experimentally, *CAP-D2* and *CAP-D3* were fused to a GS-tag and affinity-purified from Arabidopsis PSB-D suspension-cultured cells (Fig. S3). The proteins

co-purifying with *CAP-D2*-GS and *CAP-D3*-GS were identified by mass spectrometry. The putative subunits of the condensin I complex, SMC2A, SMC2B, SMC4, CAP-H and CAP-G, were detected with high scores in the *CAP-D2*-GS eluates of three affinity purifications performed. Similarly, the putative subunits of the condensin II complex, SMC2A, SMC4, CAP-H2 and CAP-G2, were detected in all three affinity purifications performed for *CAP-D3*-GS, while SMC2B was identified in two of the affinity purifications (Table 1; Fig. 1). Like in the *in silico* analysis, CAP-H and CAP-G, and CAP-H2 and CAP-G2 were

**Table 1** Arabidopsis condensin subunits predicted to interact with CAP-D2 and CAP-D3, and subunits identified by affinity purification and mass spectrometry using CAP-D2 and CAP-D3 as baits.

Predicted <i>in silico</i> (Supporting Information Fig. S2)	Identified by AP-MS	
	CAP-D2 bait	CAP-D3 bait
CAP-D2 (AT3G57060)	4539/3	-
CAP-G (AT5G37630)	1421/3	-
CAP-H (AT2G32590)	920/3	-
CAP-D3 (AT4G15890)	-	6668/3
CAP-G2 (AT1G64960)	-	218/3
CAP-H2 (AT3G16730)	-	206/3
SMC4 (AT5G48600)	2543/3	1572/3
SMC2A (AT5G62410)	2497/3	819/3
SMC2B (AT3G47460)	1932/3	503/2

The numbers indicate the average Mascot scores/number of times the interactor was detected in three independent affinity purifications. Only proteins detected in at least two purifications are listed. AP-MS, affinity purification–mass spectrometry.

identified as specific components of the condensin I and condensin II complexes, respectively, while SMC2A, SMC2B, and SMC4 co-precipitated with both CAP-D2 and CAP-D3. This analysis demonstrates that Arabidopsis, similar to mammals, chicken, and *Caenorhabditis elegans* (Onn *et al.*, 2007; Hirano, 2012a), possesses specific condensin I and II complexes. Interestingly, in addition to SMC4, both SMC2A and SMC2B may be involved in the formation of both condensin complexes.

Among the proteins which co-purified with CAP-D2 (Table S3), other proteins such as the cohesin complex subunit SMC3 were identified. Additionally, the following were found: the chromatin remodeling factors CHR17, CHR19 and CHR24; CUL1 and CUL3, subunits of the SCF ubiquitin ligase complex; HDC1, a histone deacetylase; and ELO3, a histone acetyltransferase from the Elongator complex. Among the proteins co-purifying with CAP-D3 (Table S4) were the following: two nucleosome assembly proteins NAP and CUL1; CSN1, a subunit of the COP9 signalosome (CSN); the helicase BRAHMA; ELO3, from the Elongator complex; and NERD, which is involved in DNA methylation.

### CAP-D3 organizes chromatin during interphase

The involvement of Arabidopsis CAP-D3 in keeping centromeres apart at interphase in nuclei of different ploidy levels has been described previously by Schubert *et al.* (2013). In *Drosophila*, condensin II also promotes the dispersion of pericentric heterochromatin (Bauer *et al.*, 2012). Because the T-DNA insertion could not be confirmed in any of the available T-DNA insertion lines of *CAP-D2* we screened, we focused on investigating T-DNA lines of *CAP-D3* using the two *cap-d3* mutants SAIL\_826\_B06 and *cap-d3* SALK\_094776 (Schubert *et al.*, 2013) (Fig. 4a). Arabidopsis has  $2n = 10$  chromosomes. Because the nuclei analyzed had a 4C ploidy level, that is, the DNA content of a replicated diploid nucleus, the maximum number of signals we can expect to count is ten centromeric, six 5S rDNA and

four 45S rDNA signals if these chromatin regions are completely cohesive. This is usually the case in differentiated 4C nuclei (Schubert *et al.*, 2006, 2012). Both *cap-d3* mutants showed an increased centromeric association. The nuclei showed a lower number of centromeric pAL signal clusters than wild-type. Around 80% of the *cap-d3* mutant nuclei showed less than six pAL signal clusters, while in the wild-type only 12% of nuclei had less than six signals (Figs 4b, S4). To verify that the mutation in the *CAP-D3* gene is indeed responsible for the centromeric clustering, a complementation experiment was carried out. *cap-d3* *SALK* mutant plants were transformed with a *CAP-D3\_EYFP* construct containing the coding region of *CAP-D3* fused to EYFP under the control of the 35S promoter. The centromeric association phenotype was evaluated in *cap-d3* *SALK* complemented plants by FISH and compared with the *cap-d3* *SALK* mutants and wild-type. Only 15% of the complemented nuclei showed less than six centromeric signal clusters, which is similar to the wild-type association level (Fig. 4c). This confirms that CAP-D3 is responsible for the centromere association in the mutants. In addition, the *cap-d3* mutants exhibit reduced centromeric regions compared to wild-type, based on pAL signal area measurements (Fig. S5). Arabidopsis centromeres are positioned at the nuclear periphery (Fransz *et al.*, 2002; Fang & Spector, 2005). To test whether the centromere position is influenced by the *cap-d3* mutations, nuclei were embedded in acrylamide to preserve their 3D structure followed by FISH (3D-FISH) with the centromeric pAL repeats. For each genotype – *cap-d3* *SAIL*, *cap-d3* *SALK*, and wild-type – ten nuclei were analyzed. Optical sections (3D structured illumination microscopy (3D-SIM) stacks) were acquired for each nucleus, and the centromere positions were analyzed using the ZENBLACK software tool ‘ortho view’ (Fig. 4d). In all cases, the centromeres were localized at the periphery of the nucleus, and this was also the case when centromere clustering was present in the *cap-d3* mutants (Videos S1–S3). Consequently, no deviation in the peripheral centromere positioning in wild-type and the *cap-d3* mutants occurs. Besides, no significant differences were found in the nuclear area size between the *cap-d3* mutants and wild-type plants (Fig. S6). Thus, the *cap-d3* mutations clearly induce an increased heterochromatin condensation via centromere clustering, but do not influence the nucleus size.

Besides centromeres, in Arabidopsis the 45S and 5S rDNAs are heterochromatin-associated sequences. In nuclei of differentiated cells, 45S rDNA containing nucleolar organizing regions tend to associate, but the 5S rDNA loci are often separated (Berr & Schubert, 2007). To examine whether CAP-D3 affects, in general, the organization of heterochromatin, the distribution of the 45S and 5S rDNA loci were analyzed by FISH in both *cap-d3* mutants (Fig. 5a). The majority of 45S rDNA signals are shifted from three signals in wild-type to two signals in the mutants (Fig. 5b). No difference was observed concerning 5S rDNA since > 70% of the nuclei showed between six and ten signals in the *cap-d3* mutant and wild-type plants (Fig. 5c). Thus, the *cap-d3* mutants present a higher association of the chromosomal 45S rDNA regions than the wild-type, but the number of 5S rDNA signals remains unaffected.

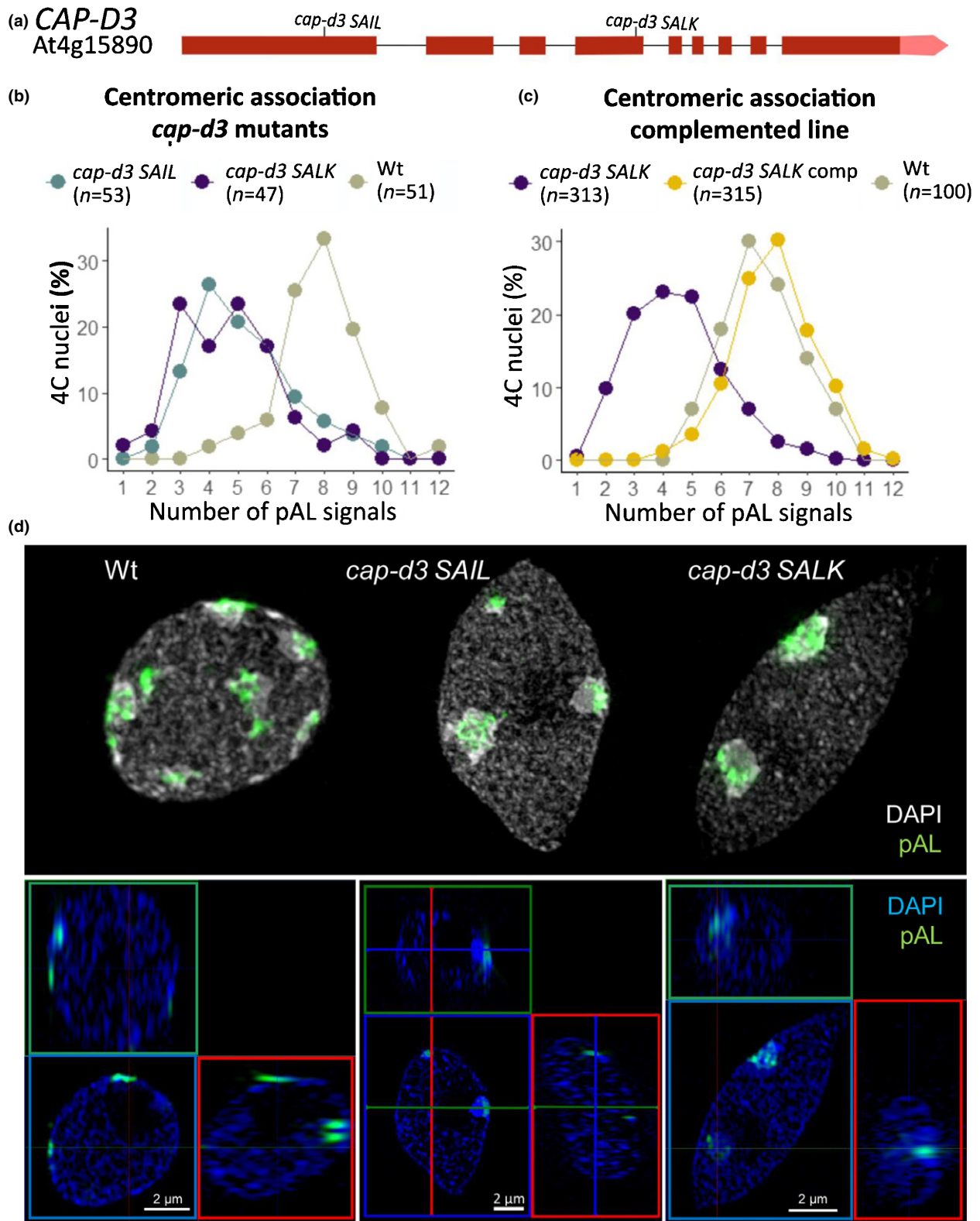


**Fig. 4** *cap-d3* mutations influence centromere association but not their spatial arrangement in Arabidopsis interphase nuclei. (a) Gene structure model of CAP-D3. Red boxes represent exons, lines represent introns, and the lighter red box represents the 3'UTR. The T-DNA insertion sites of the *cap-d3 SAIL* and *cap-d3 SALK* lines are indicated. (b, c) pAL signal frequencies in 4C nuclei of *cap-d3 SAIL*, *cap-d3 SALK*, *cap-d3 SALK* complemented, and wild-type (WT). *n*, total number of nuclei analyzed, from two different plants in (b) and from three different plants in (c). (d) 3D-SIM maximum intensity projections (upper panel) and orthogonal views (lower panel) of FISH with the centromeric repeat (pAL) on structurally preserved acrylamide-embedded 4C leaf nuclei of WT and *cap-d3* mutants. Blue, green, and red rectangles show *x*-*y*, *x*-*z* and *y*-*z* optical cross-sections, respectively.

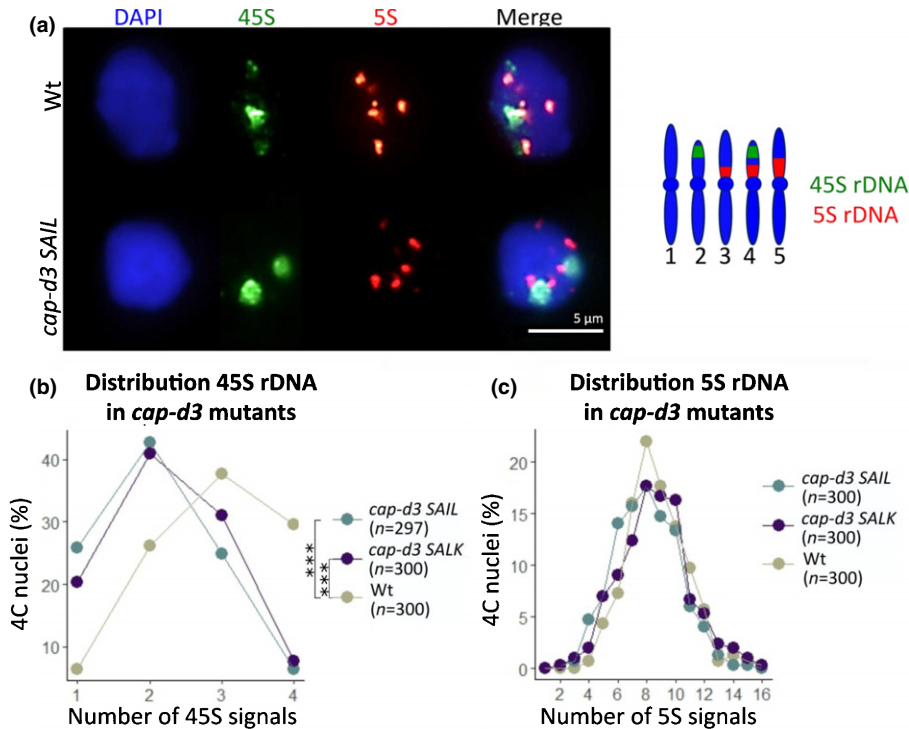


**Fig. 5** Arabidopsis *cap-d3* mutations induce 45S rDNA association but do not influence the nuclear distribution of 5S rDNA. (a) FISH signals of 45S rDNA and 5S rDNA on 4C nuclei of wild-type (WT) and *cap-d3 SAIL* mutants. The ideogram represents the Arabidopsis chromosomes, showing the localization of 45S and 5S rDNA. (b, c) Frequency of 45S and 5S rDNA signals in 4C nuclei of WT and the *cap-d3* mutants. *n*, total number of nuclei analyzed from three different plants. Differences in the number of 45S rDNA signals were statistically confirmed with the Kruskal–Wallis test and Dunn's method (\*\*\*,  $P < 0.001$ ).

### CAP-D3 does not affect the global nuclear distribution of histone marks and methylated DNA

DNA can be methylated at cytosine as 5-methyl-cytosine (5mC). The methylation of DNA is associated with heterochromatin formation, and consequently it has been found in the chromocenters of Arabidopsis (Fransz *et al.*, 2002). Mutants in which chromatin organization is affected often show a compromised distribution pattern of 5mC and histone modifications (Soppe *et al.*, 2002; Jasencakova *et al.*, 2003; Probst *et al.*, 2003; Naumann *et al.*, 2005; Tessadori *et al.*, 2007; Jacob *et al.*, 2009; Yelagandula *et al.*, 2014). To test whether such a global effect can also be observed in the *cap-d3* mutants, the distribution of methylated DNA was compared to wild-type by immunodetection of 5mC-specific sites. In both *cap-d3* mutants and wild-type, the 5mC signals were similarly chromocenter-localized (Fig. 6a). Mouse embryonic stem cells depleted of condensin show a reduction in 5mC (Fazio & Panning, 2010). The Arabidopsis centromeric repeats are highly methylated in a CpG context (Martinez-Zapater *et al.*, 1986). The use of methylation-sensitive enzymes and Southern blot hybridization allowed an additional determination of the relative DNA methylation level of the centromeric repeats. *HpaII* and its isoschizomer *MspI* cleave the same CCGG sequence, but *HpaII* is methylation-sensitive while *MspI* is not. In wild-type, the centromeric repeats are highly methylated and are thus digestible by *MspI* (Fig. 6b). The ladder-like pattern corresponds to the monomer, dimer, trimer, and higher orders of

centromeric repeats. As expected, *HpaII* does not cut in wild-type DNA. In both *cap-d3* mutants, the hybridization pattern is similar to wild-type. Thus, no major change in the relative level of CCGG methylation occurred in *cap-d3* mutants.

CAP-D3 prevents the clustering of heterochromatin, but the CAP-D3 protein itself localizes in euchromatic regions during interphase (Schubert *et al.*, 2013). Both types of chromatin are characterized by specific post-translational histone modification marks (Fuchs *et al.*, 2006). To evaluate a possible mislocalization of histone modifications in the *cap-d3* mutants, the global distribution patterns of different histone marks were compared between the *cap-d3* mutants and wild-type. Specific marks for heterochromatin (histone H3K9me1, H3K9me2) and euchromatin (histone H3K4me3, H3K27me3) were tested by indirect immunostaining. Besides, the H3 acetylation marks H3K9ac, H3K14ac and H3K18ac, as well as H3K9+14+18+23+27ac, were evaluated. Histone acetylation relaxes chromatin, allowing different protein complexes to access DNA (Wang *et al.*, 2014). In flow-sorted 4C wild-type nuclei, H3K4me3 localizes in euchromatin, and it is absent from chromocenters and the nucleolus. In *cap-d3* mutants the localization is identical. H3K9me1 is a heterochromatin-specific histone modification that localizes in the chromocenters in both *cap-d3* mutants and wild-type. Finally, the acetylation mark H3K14ac localizes mainly in euchromatin (transcriptionally active chromatin) of wild-type nuclei, but also in the mutants (Fig. 6c). The other histone modifications tested (H3K27me3, H3K9me2, H3K9ac, H3K18ac

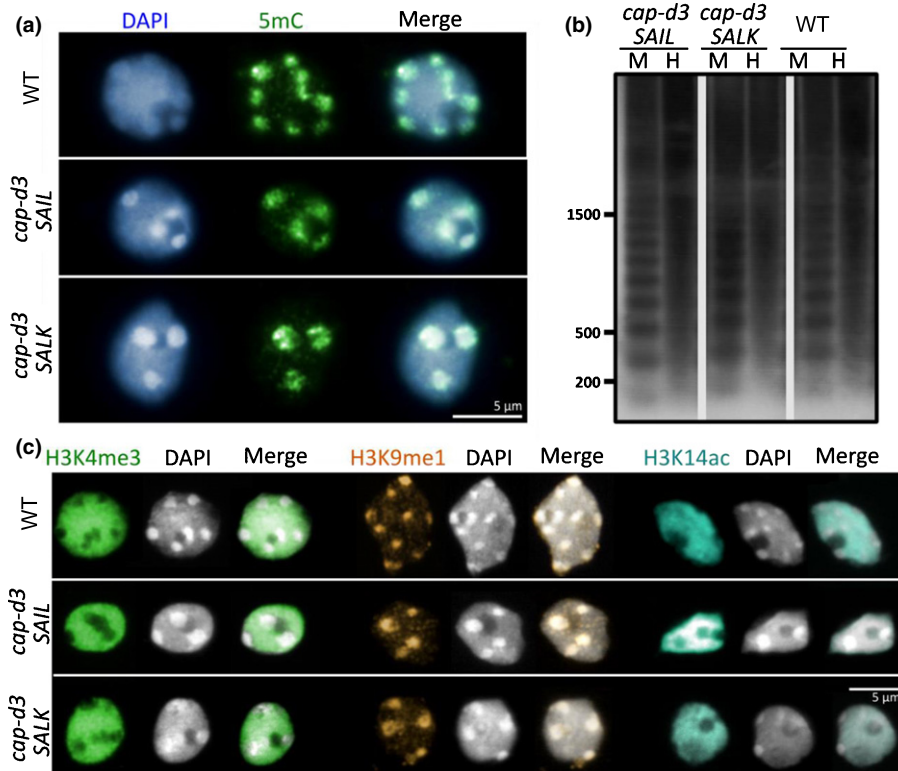


**Fig. 6** *cap-d3* mutations do not modify the epigenetic landscape in Arabidopsis interphase nuclei. (a) 5-methyl-cytosine immunolocalization on 4C nuclei of wild-type (WT) and the *cap-d3* mutants. (b) Southern blot analysis of the *cap-d3* mutants and WT genomic DNA digested with *Hpa*II (H) or *Msp*I (M) and hybridized with the P<sup>32</sup>-labeled centromeric repeat pAL does not show different digestion patterns. (c) Immunolocalization of histone H3K4me3, H3K9me1, and H3K14ac on 4C nuclei of WT and the *cap-d3* mutants. For each 5-methyl-cytosine and histone modification immunolocalization, c. 100 nuclei were checked.

and H3K14+18+23+27ac) followed the same pattern in wild-type and the *cap-d3* mutants (Fig. S7). Thus, we did not detect obvious major differences in the (sub-)nuclear distribution patterns of the different histone marks between wild-type and the *cap-d3* mutants. The influence of *cap-d3* mutations on post-translational histone modifications at the sequence level remains unknown.

### Mutation of CAP-D3 moderately affects transcription

To assess whether the mutation of *CAP-D3* affects gene transcription, the transcriptome of both *cap-d3* mutants was compared to the wild-type. RNA-sequencing was performed for four samples (pooled 4 wk-old plantlets) for each genotype. At this stage, *CAP-D2* and *CAP-D3* are transcribed in the analyzed material (Fig. S8). After differential expression analysis, we observed differences between the *cap-d3* mutants and wild-type transcriptomes. The genes with at least a two-fold change in transcription and a  $p_{Adj} \leq 0.05$  were considered to be differentially expressed genes (DEGs) between two genotypes (Fig. 7a). The smallest difference was observed between *cap-d3 SAIL* and *cap-d3 SALK* (74 DEGs), and the highest, between *cap-d3 SAIL* and wild-type (398 DEGs). *cap-d3 SALK* vs wild-type was intermediate (97 DEGs) (Fig. 7b). Both *cap-d3* mutants show centromere and 45S rDNA clustering, but *cap-d3 SAIL* plants showed additional growth defects that are absent in *cap-d3 SALK* plants. To separate

the individual effect of each allele, in the further analysis only the DEGs shared by both mutants when compared to wild-type were considered. These 83 genes, common to the *cap-d3* mutation independently of the specific alleles, are subsequently referred to as ‘*cap-d3* DEGs’ (Fig. 7b; Table S5). These genes are distributed along all chromosome arms (Fig. 7c). According to their Gene Ontology (GO) enrichment, the *cap-d3* DEGs are mainly involved in transcription, particularly in biological processes affecting the response to water, chemicals, and stress (Table 2). In agreement with their role in transcription, 13 out of the 83 *cap-d3* DEGs are transcription factors (Table S5). We conclude that the direct influence of CAP-D3 on transcription is moderate. However, the DEGs involvement in plant responses to different stimuli, and the high proportion of transcription factors, indicate that CAP-D3 may influence transcription indirectly.

### Discussion

#### Arabidopsis CAP-D proteins are expressed in cell cycle active tissues

*CAP-D2* and *CAP-D3* are highly expressed in meristems and cell cycle active tissues (flower buds, roots) but are weaker in non-cycling tissues (mature leaves). Similarly, the condensin subunit genes *CAP-H* and *SMC2* are highly expressed in dividing tissues (Liu *et al.*, 2002; Siddiqui *et al.*, 2003; Fujimoto *et al.*, 2005).

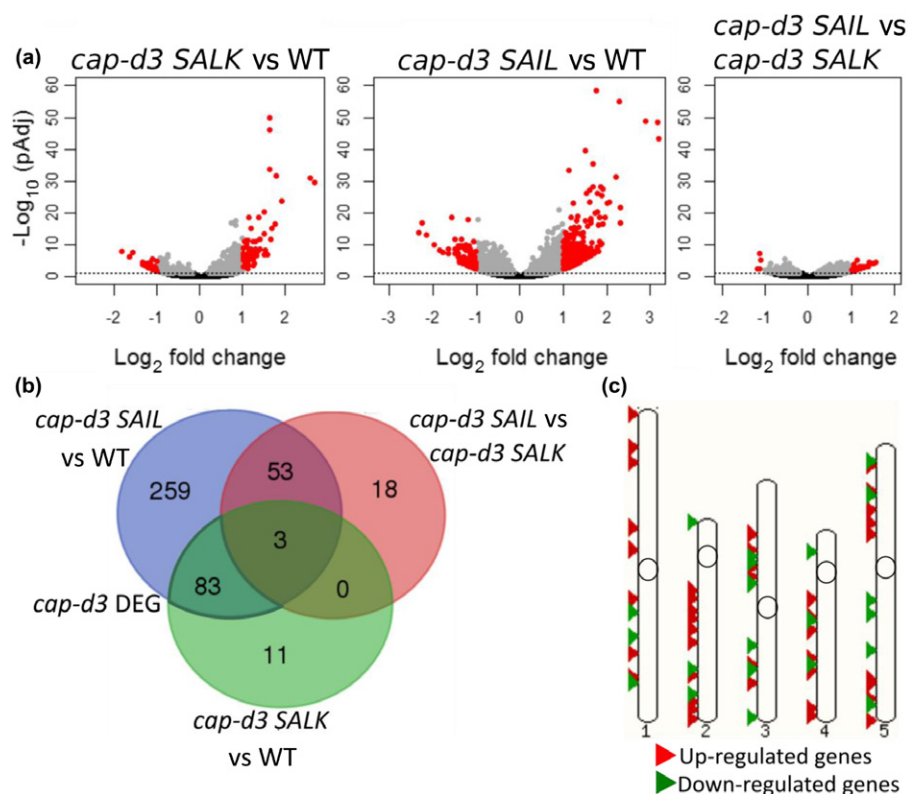


**Fig. 7** Transcriptome analysis of Arabidopsis *cap-d3* mutants and wild-type (WT) plantlets. (a) Volcano plots showing transcriptome comparisons between *cap-d3 SALK*, *cap-d3 SAIL*, and WT. The horizontal dotted line corresponds to  $\text{pAdj} = 0.05$ . Genes below are depicted in black and above in grey. The red genes are differentially expressed (DEGs) at a threshold of twofold change (i.e. upregulated:  $\geq 1 \log_2$  fold change (FC), or downregulated:  $\leq -1 \log_2$  FC) and with a  $\text{pAdj} \leq 0.05$ .  $\text{pAdj}$  is the  $P$ -value corrected for multiple testing with the Benjamini–Hochberg adjustment. (b) Venn diagram showing the DEGs across the three comparisons. Each circle comprises all the DEGs of one comparison and the intersections between circles are the common DEGs. For example, the blue circle represents the *cap-d3 SAIL vs WT* DEGs, of which there are 398; of those, 83 are the same in *cap-d3 SALK vs WT*; 53 are the same in *cap-d3 SAIL vs cap-d3 SALK*; 3 are differentially expressed in all comparisons and 259 are only present in *cap-d3 SAIL vs WT*. (c) Ideogram of Arabidopsis chromosomes showing the position of the 83 *cap-d3* DEGs along the chromosomes.

**Table 2** Gene ontology (GO) categories enriched in the 83 Arabidopsis *cap-d3* differentially expressed genes (DEGs).

Ontology	GO term	Description	FDR
Biological process	GO:0009414	Response to water deprivation	0.0001
Biological process	GO:0009415	Response to water	0.0001
Biological process	GO:0042221	Response to chemical stimulus	0.0021
Biological process	GO:0009628	Response to abiotic stimulus	0.0033
Biological process	GO:0050896	Response to stimulus	0.01
Biological process	GO:0006950	Response to stress	0.041
Molecular function	GO:0030528	Transcription regulator activity	0.024
Molecular function	GO:0003700	Transcription factor activity	0.047

FDR, false discovery rate;  $P$ -value adjusted for multiple testing.

Sequences of 391 bp and 474 bp upstream of the start of *CAP-D2* and *CAP-D3*, respectively, are sufficient to act as promoters. Longer fragments (>1000 bp) do not improve the expression of the reporter gene. Interestingly, the *CAP-D2* and *CAP-D3* promoter regions contain two previously predicted E2F binding sites

(Schubert *et al.*, 2013). E2F is a transcriptional activator of genes important for cell cycle progression. Together with the retinoblastoma-related protein (RBR) and a dimerization partner, they control the transition from G1 to S phase. E2F sites are also present in the Arabidopsis *SMC2* promoter (Siddiqui *et al.*, 2003). In mouse, *CNAP1* (*CAP-D2*) is also a target of E2F (Verlinden *et al.*, 2005). Considering the expression patterns, the promoter features, and the comparison with other organisms, it is plausible that the transcription of Arabidopsis *CAP-D2* and *CAP-D3* is cell cycle-regulated.

Introns, when affecting the expression of a gene, often enhance its expression by increasing the transcript amount or by inducing the expression in specific tissues (Rose *et al.*, 2008; Heckmann *et al.*, 2011; Parra *et al.*, 2011). Nonetheless, the second intron of *CAP-D2* could have intragenic regulatory sequences repressing the expression in nondividing tissues. This is supported herein by the loss of GUS reporter expression in leaves of the Pro3 and Pro6 transgenic plants compared with Pro2, Pro4, and Pro5 plants, which do not carry the second intron. Moreover, our RT-qPCR results showed low transcription of *CAP-D2* in mature leaves. The second intron of the *AGAMOUS* gene is also responsible for the inhibition of expression in vegetative tissues and

drives its correct expression in flowers (Sieburth & Meyerowitz, 1997).

### The subunit composition of Arabidopsis condensin I and II is similar to that in other eukaryotes

Protein immunoprecipitation (IP) from flower bud extracts has already confirmed the presence of the subunits for condensin I and condensin II in Arabidopsis (Smith *et al.*, 2014). Nonetheless, these IPs were performed with anti-SMC4, which would target both condensin complexes, and therefore could not determine the exact condensin I and condensin II composition. Our data based on affinity purification of CAP-D2 and CAP-D3 combined with mass spectrometry clarified that in Arabidopsis both condensin complexes are present and that their subunit composition is identical to those of other organisms (Hirano, 2012a). Notably, Arabidopsis is the only species in which two SMC2 homologs have been predicted and described (Siddiqui *et al.*, 2003; Cobbe & Heck, 2004). Both SMC2A and SMC2B interact with the other condensin subunits in vegetative and somatic tissues (Smith *et al.*, 2014; see second result paragraph of this study).

In human cells and *Drosophila*, CAP-D3 interacts with RBR and promotes the correct chromosomal localization of condensin II (Longworth *et al.*, 2008). In Arabidopsis, this interaction is likely not conserved, since we could not detect RBR among the proteins that co-purified with CAP-D3. In human and *Drosophila*, components of the ubiquitin-26S proteasome pathway interact and regulate condensin subunits (Buster *et al.*, 2013; Kagami *et al.*, 2017). In our affinity purifications, we also detected components of the ubiquitin-26S proteasome pathway, CUL1, CUL3 and CSN1, suggesting that in Arabidopsis, ubiquitination could be involved in the regulation of the condensins. The interaction of CAP-D2 with the cohesin subunit SMC3 suggests a combined role for both proteins; however, whether this is a *bona fide* interaction requires further confirmation.

### CAP-D3 may influence interphase chromatin arrangement and transcription, but not the global distribution of histone modifications

In *Drosophila*, CAP-D3 and CAP-H2 are required to form compact chromosomes (Hartl *et al.*, 2008; Bauer *et al.*, 2012). In Arabidopsis, previous studies based on FISH suggested an influence of CAP-D3 on the formation of interphase chromosome territories and sister chromatid cohesion (Schubert *et al.*, 2013). In addition to its role in chromosome compaction, condensin II has been described as influencing transcription in mouse, human and *Drosophila* (Longworth *et al.*, 2012; Downen *et al.*, 2013; Yuen *et al.*, 2017). The Arabidopsis *cap-d3* mutants showed transcriptional changes to a subset of genes involved in transcription and response to water, chemicals, and stress. Plants defective in other subunits of the condensin II complex are hypersensitive to stress produced by growth in boron excess and radiomimetic chemicals (zeocin and bleomycin) (Sakamoto *et al.*, 2011). The phenotypes of *cap-d3* *SAIL* and *SALK* have been described previously. Both mutations induce reduced fertility, and in the case of *SAIL* also reduced vigor

(Schubert *et al.*, 2013). Interestingly, gross chromosome rearrangements that alter the genome topology do not alter gene expression in *Drosophila* (Ghavi-Helm *et al.*, 2019). Even a budding yeast strain, after merging all 16 chromosomes into a single one, revealed a nearly identical transcriptome and similar phenome profiles as wild-type strains (Shao *et al.*, 2018). Thus, chromatin structure changes as induced in the Arabidopsis *cap-d3* mutants seem to influence the global transcription only slightly.

Wang *et al.* (2017) showed that Arabidopsis SMC4, but not CAP-D3, is important for the maintenance of the repression of pericentromeric retrotransposons independent of DNA methylation. Accordingly, we observed no increased retrotransposon transcription in any of the *cap-d3* mutants. The protein-coding genes upregulated in *smc4* mutants are mainly involved in flower development, reproductive processes, and DNA repair, and are distributed all over the genome (Wang *et al.*, 2017). However, we observed in the *cap-d3* mutants a differential expression of genes involved in transcription and stress response. This difference could be due to the combined effects of both the condensin I and II complexes in the *smc4* mutants, while in our *cap-d3* mutants only condensin II is compromised.

Posttranslational histone modifications may affect the structure and stiffness of interphase nuclei, and decondensed euchromatin correlates with less rigid nuclei (Chalut *et al.*, 2012; Krause *et al.*, 2013; Haase *et al.*, 2016). In human HeLa cells histone methylation, but not acetylation, contributes to the stiffness and structure of condensed mitotic chromosomes (Biggs *et al.*, 2019). Histone acetylation relaxes chromatin, allowing different protein complexes to access DNA. Thus, acetylation is associated with transcription, and hypoacetylation with transcriptional repression (Wang *et al.*, 2014).

It seems that the unaltered pattern of histone acetylation reflects only a moderate effect on transcription, as we observed in the *cap-d3* mutants.

### CAP-D prevents clustering of heterochromatin

CAP-H2 promotes the spatial separation of heterochromatic regions in *Drosophila* during interphase (Bauer *et al.*, 2012; Buster *et al.*, 2013). Correspondingly, in Arabidopsis, depletion of CAP-D3 results in centromere clustering in 2C, 4C, and 8C interphase nuclei (Schubert *et al.*, 2013). We confirmed this phenotype in 4C nuclei and found that CAP-D3 depletion also results in the clustering of the 45S rDNA loci but not of the 5S rDNA sites. Differential behavior of rDNA was also found in protoplasts of Arabidopsis. 45S rDNA remains condensed while the 5S rDNA decondensed during protoplast formation (Tessadori *et al.*, 2007). 5S and 45S rDNA are transcribed by RNA polymerases III and I, respectively (Layat *et al.*, 2012). Therefore, the different clustering behaviors of both rDNAs in the *cap-d3* mutants could be due to their different structural and functional properties. Otherwise, in yeast, condensin is enriched at RNA polymerase III genes to cluster them (D'Ambrosio *et al.*, 2008; Haeusler *et al.*, 2008). Whether the smaller genome size of yeast might be responsible or whether the yeast condensin, which is, for the most part, similar to plant condensin I (Freeman *et al.*,

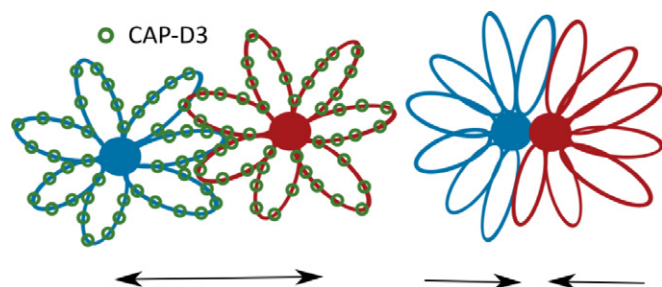


**Fig. 8** A model explaining the function of Arabidopsis CAP-D3 in interphase nuclei. Two chromosomes are represented in blue and in red, with euchromatin emanating loops from their pericentromeric chromocenters (rosette chromosome model; Fransz *et al.*, 2002; De Nooijer *et al.*, 2009). CAP-D3 (green circles) localizes along euchromatin, creating the rigid chromatin loops required to keep the chromocenters separated (left). In absence of CAP-D3, the chromatin loops are not stiff enough to counterbalance the depletion-attraction forces (Marenduzzo *et al.*, 2006). Consequently, the chromocenters cluster (right).

2000; Hirano, 2012a), may cause the difference is an interesting question to address in order to clarify whether condensin has an additional role for organizing the larger plant genomes.

Chromocenters are chromatin structures that can be intensely stained by DNA-specific dyes and represent condensed heterochromatin regions in interphase nuclei (Jost *et al.*, 2012). In Arabidopsis chromocenters are located near the nuclear periphery, and they incarnate centromeric and pericentromeric heterochromatin, the 45S rDNA, and the 5S rDNA (Fransz *et al.*, 2002; Schubert *et al.*, 2012). The nuclear and chromocenter phenotype which we observed in the *cap-d3* mutants differs from previous reports of proteins important for the maintenance of the chromocenters (Moissiard *et al.*, 2012; Sakamoto & Takagi, 2013; Wang *et al.*, 2013; Tatout *et al.*, 2014; Poulet *et al.*, 2017). The chromocenters cluster and localize at the nuclear periphery, but they do not decondense, the nuclear area does not change compared to that of wild-type, and the general degree of DNA and histone methylation is unaffected. Moreover, CAP-D3 has little effect on transcriptional silencing, because no increased transcription of transposable elements was detected in *cap-d3* mutants (Wang *et al.*, 2017). MORC, CRWN, and LINC proteins localize close to the chromocenters (Moissiard *et al.*, 2012; Sakamoto & Takagi, 2013; Tatout *et al.*, 2014). Conversely, CAP-D3 influences the arrangement of the chromocenters but localizes exclusively in euchromatin during interphase (Schubert *et al.*, 2013). Therefore, CAP-D3 has a mostly structural role during interphase and affects the clustering of chromocenters without localizing close to them.

Previous statistical analyses have detected more regular, rather than a completely random, spatial centromere and chromocenter distributions in animal and plant nuclei. This suggests that repulsive constraints or spatial inhomogeneities influence the 3D organization of heterochromatin (Andrey *et al.*, 2010). Computer simulation modeling of Arabidopsis chromosomes as polymers predicts that the position of the chromocenters in the nucleus is due to nonspecific interactions (De Nooijer *et al.*, 2009). The simulated chromosomes exhibit chromocenter clustering, except for the so-called rosette chromosomes (Fransz *et al.*, 2002), in

which the euchromatin loops emanate from the chromocenter and thus prevent chromocenter clustering. Indeed, depletion-attraction forces predict that big particles in an environment crowded with small particles will tend to cluster together (Marenduzzo *et al.*, 2006). This situation can be applied to the nucleus, where the chromocenters act as big particles and euchromatin as small particles. If the association is not prevented, the chromocenters will cluster.

We suppose that during interphase CAP-D3 localizes in euchromatin, possibly along with euchromatic loops, mediating the rigidity which is needed to keep the chromocenters away from each other. In the case of lacking or functionally impaired CAP-D3, the loops may be not stiff enough to prevent the chromocenter clustering (Fig. 8). The finding that condensed chromatin resists mechanical forces, whereas decondensed chromatin is softer (Maeshima *et al.*, 2018), supports the idea that the stiffness of chromatin is an important feature for the organization of cell nuclei. Our observation that the distribution patterns of DNA and histone methylation and histone acetylation are not altered in the *cap-d3* mutants suggests that these post-translational histone modifications are possibly not required for the rigidity of interphase chromosome territory structures.

## Acknowledgements

We thank Jörg Fuchs for flow-sorting of nuclei, Katrin Kumke, Oda Weiss, and Karla Meier for excellent technical assistance, Axel Himmelbach for sequencing, and Ingo Schubert for critical reading of the manuscript. The work was supported by a Marie Curie Initial Training Network fellowship (FP7-PEOPLE-2013-ITN, CHIP-ET). The A. Bruckmann and KDG laboratories were supported by the German Research Foundation through grant SFB960. IL was supported by European Regional Development 'Fund-Project MSCAfellow@MUNI' (no. CZ.02.2.69/0.0/0.0/17\_050/0008496). The authors have no conflicts of interest to report. Open access funding enabled and organized by Projekt DEAL.

## Author contributions

VS, CM, AH, and KG conceived the study and designed the experiments. AH and VS contributed equally to supervision of the project. CM, WA, KZ, and VS performed the experiments. CM, EK, MVB, IE, FC, ABräutigam, ABruckmann, and IL performed the bioinformatic analysis. CM and VS wrote the manuscript. All authors read and approved the final manuscript.

## ORCID

Wojciech Antosz  <https://orcid.org/0000-0001-9127-8267>  
 Andrea Bräutigam  <https://orcid.org/0000-0002-5309-0527>  
 Astrid Bruckmann  <https://orcid.org/0000-0001-6082-2944>  
 Frederik Coppens  <https://orcid.org/0000-0001-6565-5145>  
 Ignacio Eguinoa  <https://orcid.org/0000-0002-6190-122X>  
 Klaus D. Grasser  <https://orcid.org/0000-0002-7080-5520>  
 Andreas Houben  <https://orcid.org/0000-0003-3419-239X>  
 Etienne Kornobis  <https://orcid.org/0000-0001-7712-8270>

Inna Lermontova  <https://orcid.org/0000-0003-3386-2590>  
Celia Municio  <https://orcid.org/0000-0002-0788-1520>  
Veit Schubert  <https://orcid.org/0000-0002-3072-0485>  
Michiel Van Bel  <https://orcid.org/0000-0002-1873-2563>

## Data availability

The data that support the findings of this study are openly available in the European Nucleotide Archive at <https://www.ebi.ac.uk/ena>, ArrayExpress accession E-MTAB-8969.

## References

- Afgan E, Baker D, Batut B, Van Den Beek M, Bouvier D, Čech M, Chilton J, Clements D, Coraor N, Grüning BA *et al.* 2018. The Galaxy platform for accessible, reproducible and collaborative biomedical analyses: 2018 update. *Nucleic Acids Research* 46: W537–W544.
- Anders S, Pyl PT, Huber W. 2015. HTSeq - a Python frame work to work with high-throughput sequencing data. *Bioinformatics* 31: 166–169.
- Andrey P, Kieu K, Kress C, Lehmann G, Tirichine L, Liu ZC, Biot E, Adenot PG, Hue-Beauvais C, Houba-Herlin N *et al.* 2010. Statistical analysis of 3D images detects regular spatial distributions of centromeres and chromocenters in animal and plant nuclei. *PLoS Computational Biology* 6: e1000853.
- Antosz W, Pfab A, Ehrnsberger HF, Holzinger P, Kollen K, Mortensen SA, Bruckmann A, Schubert T, Langst G, Griesenbeck J *et al.* 2017. The composition of the Arabidopsis RNA polymerase II transcript elongation complex reveals the interplay between elongation and mRNA processing factors. *The Plant Cell* 29: 854–870.
- Bauer CR, Hartl TA, Bosco G. 2012. Condensin II promotes the formation of chromosome territories by inducing axial compaction of polyploid interphase chromosomes. *PLoS Genetics* 8: e1002873.
- Berr A, Schubert I. 2007. Interphase chromosome arrangement in *Arabidopsis thaliana* is similar in differentiated and meristematic tissues and shows a transient mirror symmetry after nuclear division. *Genetics* 176: 853–863.
- Biggs R, Liu PZ, Stephens AD, Marko JF. 2019. Effects of altering histone posttranslational modifications on mitotic chromosome structure and mechanics. *Molecular Biology of the Cell* 30: 820–827.
- Bolger AM, Lohse M, Usadel B. 2014. Trimmomatic: a flexible trimmer for Illumina sequence data. *Bioinformatics* 30: 2114–2120.
- Buster DW, Daniel SG, Nguyen HQ, Windler SL, Skwarek LC, Peterson M, Roberts M, Meserve JH, Hartl T, Klebba JE *et al.* 2013. SCFslimb ubiquitin ligase suppresses condensin II-mediated nuclear reorganization by degrading Cap-H2. *Journal of Cell Biology* 201: 49–63.
- Campbell BR, Song Y, Posch TE, Cullis CA, Town CD. 1992. Sequence and organization of 5S ribosomal RNA-encoding genes of *Arabidopsis thaliana*. *Gene* 112: 225–228.
- Chalut KJ, Hopfler M, Lautenschlager F, Boyde L, Chan CJ, Ekpenyong A, Martinez-Arias A, Guck J. 2012. Chromatin decondensation and nuclear softening accompany Nanog downregulation in embryonic stem cells. *Biophysical Journal* 103: 2060–2070.
- Clough SJ, Bent AF. 1998. Floral dip: A simplified method for Agrobacterium-mediated transformation of *Arabidopsis thaliana*. *The Plant Journal* 16: 735–743.
- Cobbe N, Heck MMS. 2004. The evolution of SMC proteins: phylogenetic analysis and structural implications. *Molecular Biology and Evolution* 21: 332–347.
- D'Ambrosio C, Schmidt CK, Katou Y, Kelly G, Itoh T, Shirahige K, Uhlmann F. 2008. Identification of cis-acting sites for condensin loading onto budding yeast chromosomes. *Genes and Development*, 22: 2215–2227.
- De Nooijer S, Wellink J, Mulder B, Bisseling T 2009. Non-specific interactions are sufficient to explain the position of heterochromatic chromocenters and nucleoli in interphase nuclei. *Nucleic Acids Research* 37: 3558–3568.
- Downen JM, Bilodeau S, Orlando DA, Hübner MR, Abraham BJ, Spector DL, Young RA. 2013. Multiple structural maintenance of chromosome complexes at transcriptional regulatory elements. *Stem Cell Reports* 1: 371–378.
- Du Z, Zhou X, Ling Y, Zhang Z, Su Z. 2010. agriGO: a GO analysis toolkit for the agricultural community. *Nucleic Acids Research* 38: W64–W70.
- Dürr J, Lolas IB, Sørensen BB, Schubert V, Houben A, Melzer M, Deutzmann R, Grasser M, Grasser KD. 2014. The transcript elongation factor SPT4/SPT5 is involved in auxin-related gene expression in *Arabidopsis*. *Nucleic Acids Research* 42: 4332–4347.
- Elbatsh AMO, Kim E, Eeftens JM, Raaijmakers JA, van der Weide RH, Garcia-Nieto A, Bravo S, Ganji M, Uit de Bos J, Teunissen H *et al.* 2019. Distinct roles for condensin's two ATPase sites in chromosome condensation. *Molecular Cell* 76: 1–14.
- Fang Y, Spector DL. 2005. Centromere positioning and dynamics in living *Arabidopsis* plants. *Molecular Biology of the Cell* 16: 5710–5718.
- Fazio TG, Panning B. 2010. Condensin complexes regulate mitotic progression and interphase chromatin structure in embryonic stem cells. *Journal of Cell Biology* 188: 491–503.
- Franz P, de Jong JH, Lysak M, Castiglione MR, Schubert I. 2002. Interphase chromosomes in *Arabidopsis* are organized as well defined chromocenters from which euchromatin loops emanate. *Proceedings of the National Academy of Sciences, USA* 99: 14584–14589.
- Freeman L, Aragon-Alcaide L, Strunnikov A. 2000. The condensin complex governs chromosome condensation and mitotic transmission of rDNA. *Journal of Cell Biology* 149: 811–824.
- Fuchs J, Demidov D, Houben A, Schubert I. 2006. Chromosomal histone modification patterns – from conservation to diversity. *Trends in Plant Science* 11: 199–208.
- Fujimoto S, Yonemura M, Matsunaga S, Nakagawa T, Uchiyama S, Fukui K. 2005. Characterization and dynamic analysis of *Arabidopsis* condensin subunits, AtCAP-H and AtCAP-H2. *Planta* 222: 293–300.
- Gerlich D, Hirota T, Koch B, Peters JM, Ellenberg J. 2006. Condensin I stabilizes chromosomes mechanically through a dynamic interaction in live cells. *Current Biology* 16: 333–344.
- Ghavi-Helm Y, Jankowski A, Meiers S, Viales R, Korbel JO, Furlong EM. 2019. Highly rearranged chromosomes reveal uncoupling between genome topology and gene expression. *Nature Genetics* 51: 1272–1282.
- Gibus JH, Samejima K, Goloborodko A, Samejima I, Naumova N, Nuebler J, Kanemaki MT, Xie L, Paulson JR, Pearnshaw WC *et al.* 2018. A pathway for mitotic chromosome formation. *Science* 359: 652.
- Green LC, Kalitsis P, Chang TM, Cipetic M, Kim JH, Marshall O, Turnbull L, Whitchurch CB, Vagnarelli P, Samejima K *et al.* 2012. Contrasting roles of condensin I and condensin II in mitotic chromosome formation. *Journal of Cell Science* 125: 1591–1604.
- Haase K, Macadangdang JK, Edrington CH, Cuerrier CM, Hadjiantoniou S, Harden JL, Skerjanc IS, Pelling AE. 2016. Extracellular forces cause the nucleus to deform in a highly controlled anisotropic manner. *Scientific Reports* 6: 21300.
- Haeusler RA, Pratt-Hyatt M, Good PD, Gipson TA, Engelke DR. 2008. Clustering of yeast tRNA genes is mediated by specific association of condensin with tRNA gene transcription complexes. *Genes & Development* 22: 2204–2214.
- Hartl TA, Sweeney SJ, Knepler PJ, Bosco G. 2008. Condensin II resolves chromosomal associations to enable anaphase I segregation in *Drosophila* male meiosis. *PLoS Genetics* 4: 18–22.
- Heckmann S, Lermontova I, Berckmans B, de Veylder L, Bäumlein H, Schubert I. 2011. The E2F transcription factor family regulates CENH3 expression in *Arabidopsis thaliana*. *The Plant Journal* 68: 646–656.
- Herzog S, Jaiswal SN, Urban E, Riemer A, Fischer S, Heidmann SK. 2013. Functional dissection of the *Drosophila melanogaster* condensin subunit Cap-G reveals its exclusive association with condensin I. *PLoS Genetics* 9: e1003463.
- Hirano T. 2012a. Condensins: universal organizers of chromosomes with diverse functions. *Genes & Development* 26: 1659–1678.
- Hirano T. 2012b. Chromosome territories meet a condensin. *PLoS Genetics* 8: e1002939.
- Hirota T, Gerlich D, Koch B, Ellenberg J, Peters JM. 2004. Distinct functions of condensin I and II in mitotic chromosome assembly. *Journal of Cell Science* 117: 6435–6445.
- Hudson DF, Vagnarelli P, Gassmann R, Earnshaw WC. 2003. Condensin is required for nonhistone protein assembly and structural integrity of vertebrate mitotic chromosomes. *Developmental Cell* 5: 323–336.

- Jacob Y, Feng S, LeBlanc CA, Bernatavichute YV, Stroud H, Cokus S, Johnson LM, Pellegrini M, Jacobsen SE, Michaels SD. 2009. ATXR5 and ATXR6 are H3K27 monomethyltransferases required for chromatin structure and gene silencing. *Nature Structural & Molecular Biology* 16: 763–768.
- Jasencakova Z, Soppe WJJ, Meister A, Gernand D, Turner BM, Schubert I. 2003. Histone modifications in Arabidopsis – High methylation of H3 lysine 9 is dispensable for constitutive heterochromatin. *The Plant Journal* 33: 471–480.
- Jefferson RA, Kavanagh TA, Bevan MW. 1987. GUS fusions: beta-glucuronidase as a sensitive and versatile gene fusion marker in higher plants. *EMBO Journal* 6: 3901–3907.
- Jeppsson K, Kanno T, Shirahige K, Sjögren C. 2014. The maintenance of chromosome structure: positioning and functioning of SMC complexes. *Nature Reviews Molecular Cell Biology* 15: 601–614.
- Jost KL, Bertulat B, Cardoso MC. 2012. Heterochromatin and gene positioning: inside, outside, any side? *Chromosoma* 121: 555–563.
- Kagami Y, Ono M, Yoshida K. 2017. Plk1 phosphorylation of CAP-H2 triggers chromosome condensation by condensin II at the early phase of mitosis. *Scientific Reports* 7: 5583.
- Kikuchi S, Kishii M, Shimizu M, Tsujimoto H. 2005. Centromere-specific repetitive sequences from *Torenia*, a model plant for interspecific fertilization, and whole-mount FISH of its interspecific hybrid embryos. *Cytogenetics and Genome Research* 109: 228–235.
- Krause M, Te Riet J, Wolf K. 2013. Probing the compressibility of tumor cell nuclei by combined atomic force-confocal microscopy. *Physical Biology* 10: 065002.
- Kudo T, Sasaki Y, Terashima S, Matsuda-Imai N, Takano T, Saito M, Kanno M, Ozaki S, Suwabe K, Suzuki G *et al.* 2016. Identification of reference genes for quantitative expression analysis using large-scale RNA-seq data of *Arabidopsis thaliana* and model crop plants. *Genes & Genetic Systems* 91: 111–125.
- Layat E, Sáez-Vásquez J, Tourmente S. 2012. Regulation of pol I-transcribed 45S rDNA and pol III-transcribed 5S rDNA in Arabidopsis. *Plant and Cell Physiology* 53: 267–276.
- Lermontova I, Rutten T, Schubert I. 2011. Deposition, turnover, and release of CENH3 at *Arabidopsis* centromeres. *Chromosoma* 120: 633–640.
- Liu CM, McElver J, Tzafir I, Joosen R, Wittich P, Patton D, van Lammeren AAM, Meinke D. 2002. Condensin and cohesin knockouts in *Arabidopsis* exhibit a *titan* seed phenotype. *The Plant Journal* 29: 405–415.
- Livak KJ, Schmittgen TD. 2001. Analysis of relative gene expression data using real-time quantitative PCR and the 2<sup>-ΔΔC<sub>T</sub></sup> method. *Methods* 25: 402–408.
- Longworth MS, Herr A, Ji JY, Dyson NJ. 2008. RBF1 promotes chromatin condensation through a conserved interaction with the Condensin II protein dCAP-D3. *Genes & Development* 22: 1011–1024.
- Longworth MS, Walker JA, Anderssen E, Moon NS, Gladden A, Heck MMS, Ramaswamy S, Dyson NJ. 2012. A shared role for RBF1 and dCAP-D3 in the regulation of transcription with consequences for innate immunity. *PLoS Genetics* 8: e1002618.
- Love MI, Huber W, Anders S. 2014. Moderated estimation of fold change and dispersion for RNA-seq data with DESeq2. *Genome Biology* 15: 550.
- Maeshima K, Laemmli UK. 2003. A two-step scaffolding model for mitotic chromosome assembly. *Developmental Cell* 4: 467–480.
- Maeshima K, Tamura S, Shimamoto Y. 2018. Chromatin as a nuclear spring. *Biophysics and Physicobiology* 15: 189–195.
- Marenduzzo D, Finan K, Cook PR. 2006. The depletion attraction: An underappreciated force driving cellular organization. *Journal of Cell Biology* 175: 681–686.
- Martinez-Zapater JM, Estelle MA, Somerville CR. 1986. A highly repeated DNA sequence in *Arabidopsis thaliana*. *Molecular Genetics and Genomics* 204: 417–423.
- Moissiard G, Cokus SJ, Cary J, Feng S, Billi AC, Stroud H, Husmann D, Zhan Y, Lajoie BR, McCord RP *et al.* 2012. MORC family ATPases required for heterochromatin condensation and gene silencing. *Science* 336: 1448–1451.
- Nakamura S, Mano S, Tanaka Y, Ohnishi M, Nakamori C, Araki M, Niwa T, Nishimura M, Kaminaka H, Nakagawa T *et al.* 2010. Gateway binary vectors with the bialaphos resistance gene, *bar*, as a selection marker for plant transformation. *Bioscience, Biotechnology, and Biochemistry* 74: 1315–1319.
- Nasmyth K, Haering C. 2005. The structure and function of SMC and kleisin complexes. *Annual Review of Biochemistry* 74: 595–648.
- Naumann K, Fischer A, Hofmann I, Krauss V, Phalke S, Irmeler K, Hause G, Aurich AC, Dorn R, Jenuwein T *et al.* 2005. Pivotal role of AtSUVH2 in heterochromatic histone methylation and gene silencing in *Arabidopsis*. *EMBO Journal* 24: 1418–1429.
- Onn I, Aono N, Hirano M, Hirano T. 2007. Reconstitution and subunit geometry of human condensin complexes. *EMBO Journal* 26: 1024–1034.
- Ono T, Fang Y, Spector DL, Hirano T. 2004. Spatial and temporal regulation of condensins I and II in mitotic chromosome assembly in human cells. *Molecular Biology of the Cell* 15: 3296–3308.
- Ono T, Losada A, Hirano M, Myers MP, Neuwald AF, Hirano T. 2003. Differential contributions of condensin I and condensin II to mitotic chromosome architecture in vertebrate cells. *Cell* 115: 109–121.
- Parra G, Bradnam K, Rose AB, Korf I. 2011. Comparative and functional analysis of intron-mediated enhancement signals reveals conserved features among plants. *Nucleic Acids Research* 39: 5328–5337.
- Pecinka A, Schubert V, Meister A, Kreth G, Klatte M, Lysak MA, Fuchs J, Schubert I. 2004. Chromosome territory arrangement and homologous pairing in nuclei of *Arabidopsis thaliana* are predominantly random except for NOR-bearing chromosomes. *Chromosoma* 113: 258–269.
- Poulet A, Duc C, Voisin M, Desset S, Tutois S, Vanrobays E, Benoit M, Evans DE, Probst AV, Tatout C. 2017. The LINC complex contributes to heterochromatin organisation and transcriptional gene silencing in plants. *Journal of Cell Science* 130: 590–601.
- Probst AV, Franz PF, Paszkowski J, Mittelsten SO. 2003. Two means of transcriptional reactivation within heterochromatin. *The Plant Journal* 33: 743–749.
- Rose AB, Elfersi T, Parra G, Korf I. 2008. Promoter-proximal introns in *Arabidopsis thaliana* are enriched in dispersed signals that elevate gene expression. *The Plant Cell* 20: 543–551.
- Rosin LF, Nguyen SC, Joyce EF. 2018. Condensin II drives large-scale folding and spatial partitioning of interphase chromosomes in *Drosophila* nuclei. *PLoS Genetics* 14: e1007393.
- Sakamoto T, Inui YT, Uruguchi S, Yoshizumi T, Matsunaga S, Mastui M, Umeda M, Fukui K, Fujiwara T. 2011. Condensin II alleviates DNA damage and is essential for tolerance of boron overload stress in *Arabidopsis*. *The Plant Cell* 23: 3533–3546.
- Sakamoto T, Sugiyama T, Yamashita T, Matsunaga S. 2019. Plant condensin II is required for the correct spatial relationship between centromeres and rDNA arrays. *Nucleus* 10: 116–125.
- Sakamoto Y, Takagi S. 2013. LITTLE NUCLEI 1 and 4 regulate nuclear morphology in *Arabidopsis thaliana*. *Plant and Cell Physiology* 54: 622–633.
- Savvidou E, Cobbe N, Steffensen S, Cotterill S, Heck MMS. 2005. *Drosophila* CAP-D2 is required for condensin complex stability and resolution of sister chromatids. *Journal of Cell Science* 118: 2529–2543.
- Schneider CA, Rasband WS, Eliceiri KW. 2012. NIH Image to ImageJ: 25 years of image analysis. *Nature Methods* 9: 671–675.
- Schubert V. 2009. SMC proteins and their multiple functions in higher plants. *Cytogenetics and Genome Research* 124: 202–214.
- Schubert V, Berr A, Meister A. 2012. Interphase chromatin organisation in *Arabidopsis* nuclei: constraints versus randomness. *Chromosoma* 121: 369–387.
- Schubert V, Klatte M, Pecinka A, Meister A, Jasencakova Z, Schubert I. 2006. Sister chromatids are often incompletely aligned in meristematic and endopolyploid interphase nuclei of *Arabidopsis thaliana*. *Genetics* 172: 467–475.
- Schubert V, Lermontova I, Schubert I. 2013. The Arabidopsis CAP-D proteins are required for correct chromatin organisation, growth and fertility. *Chromosoma* 122: 517–533.
- Shao Y, Lu N, Wu Z, Cai C, Wang S, Zhang L, Zhou F, Xiao S, Liu L, Zeng X *et al.* 2018. Creating a functional single-chromosome yeast. *Nature* 560: 331–335.
- Siddiqui NU, Stronghill PE, Dengler RE, Hasenkamp A, Riggs CD. 2003. Mutations in *Arabidopsis* condensin genes disrupt embryogenesis, meristem organization and segregation of homologous chromosomes during meiosis. *Development* 130: 3283–3295.
- Sieburth LE, Meyerowitz EM. 1997. Molecular dissection of the AGAMOUS control region shows that cis elements for spatial regulation are located intragenically. *The Plant Cell* 9: 355–365.
- Skibbens RV. 2019. Condensins and cohesins – one of these things is not like the other! *Journal of Cell Science* 132: jcs220491.

- Smith SJ, Osman K, Franklin FCH. 2014. The condensin complexes play distinct roles to ensure normal chromosome morphogenesis during meiotic division in *Arabidopsis*. *The Plant Journal* **80**: 255–268.
- Soppe WJJ, Jasencakova Z, Houben A, Kakutani T, Meister A, Huang MS, Jacobsen SE, Schubert I, Fransz PF. 2002. DNA methylation controls histone H3 lysine 9 methylation and heterochromatin assembly in *Arabidopsis*. *EMBO Journal* **21**: 6549–6559.
- Szklarczyk D, Gable AL, Lyon D, Junge A, Wyder S, Huerta-Cepas J, Simonovic M, Doncheva NT, Morris JH, Bork P *et al.* 2019. STRING v11: protein–protein association networks with increased coverage, supporting functional discovery in genome-wide experimental datasets. *Nucleic Acids Research* **47**: D607–D613.
- Tatout C, Evans DE, Vanrobays E, Probst AV, Graumann K. 2014. The plant LINC complex at the nuclear envelope. *Chromosome Research* **22**: 241–252.
- Tessadori F, Chupeau MC, Chupeau Y, Knip M, Germann S, van Driel R, Fransz P, Gaudin V. 2007. Large-scale dissociation and sequential reassembly of pericentric heterochromatin in dedifferentiated *Arabidopsis* cells. *Journal of Cell Science* **120**: 1200–1208.
- Van Leene J, Eeckhout D, Cannoot B, De Winne N, Persiau G, Van De Slijke E, Vercruyse L, Dedeker M, Verkest A, Vandepoele K *et al.* 2015. An improved toolbox to unravel the plant cellular machinery by tandem affinity purification of *Arabidopsis* protein complexes. *Nature Protocols* **10**: 169–187.
- Van Ruiten MS, Rowland BD. 2018. SMC Complexes: universal DNA looping machines with distinct regulators. *Trends in Genetics* **34**: 477–487.
- Verlinden L, Eelen G, Beullens I, Van Camp M, Van Hummelen P, Engelen K, Van Hellemont R, Marchal K, De Moor B, Fijter F *et al.* 2005. Characterization of the condensin component Cnap1 and protein kinase melk as novel E2F target genes down-regulated by 1,25-dihydroxyvitamin D3. *Journal of Biological Chemistry* **280**: 37319–37330.
- Wallace HA, Bosco G. 2013. Condensins and 3D organization of the interphase nucleus. *Current Genetic Medicine Reports* **1**: 219–229.
- Wallace HA, Klebba JE, Kusch T, Rogers GC, Bosco G. 2015. Condensin II regulates interphase chromatin organization through the Mrg-binding motif of Cap-H2. *G3: Genes, Genomes, Genetics* **5**: 803–817.
- Walther N, Hossain MJ, Politi AZ, Koch B, Kueblbeck M, Odegard-Fougner O, Lampe M, Ellenberg J. 2018. A quantitative map of human condensins provides new insights into mitotic chromosome architecture. *Journal of Cell Biology* **217**: 2309–2328.
- Wang H, Dittmer TA, Richards EJ. 2013. *Arabidopsis* CROWDED NUCLEI (CRWN) proteins are required for nuclear size control and heterochromatin organization. *BMC Plant Biology* **13**: 200.
- Wang J, Blevins T, Podicheti R, Haag JR, Tan EH, Wang F, Pikaard CS. 2017. Mutation of *Arabidopsis* SMC4 identifies condensin as a corepressor of pericentromeric transposons and conditionally expressed genes. *Genes & Development* **31**: 1601–1614.
- Wang Z, Cao H, Chen F, Liu Y. 2014. The roles of histone acetylation in seed performance and plant development. *Plant Physiology and Biochemistry* **84**: 125–133.
- Weisshart K, Fuchs J, Schubert V. 2016. Structured illumination microscopy (SIM) and photoactivated localization microscopy (PALM) to analyze the abundance and distribution of RNA polymerase II molecules on flow-sorted *Arabidopsis* nuclei. *Bio-Protocol* **6**: e1725.
- Wu TD, Nacu S. 2010. Fast and SNP-tolerant detection of complex variants and splicing in short reads. *Bioinformatics* **26**: 873–881.
- Yelagandula R, Stroud H, Holec S, Zhou K, Feng S, Zhong X, Muthurajan UM, Nie X, Kawashima T, Groth M *et al.* 2014. The histone variant H2A.W defines heterochromatin and promotes chromatin condensation in *Arabidopsis*. *Cell* **158**: 98–109.
- Yilmaz A, Mejia-Guerra MK, Kurz K, Liang X, Welch L, Grotewold E. 2011. AGRIS: the *Arabidopsis* gene regulatory information server, an update. *Nucleic Acids Research* **39**: D1118–D1122.
- Yuen KC, Slaughter BD, Gerton JL. 2017. Condensin II is anchored by TFIIC and H3K4me3 in the mammalian genome and supports the expression of active dense gene clusters. *Science Advances*. **3**: e1700191.
- Zelkowsky M, Zelkowska K, Conrad U, Hesse S, Lermontova I, Marzec M, Meister A, Houben A, Schubert V. 2019. *Arabidopsis* NSE4 proteins act in somatic nuclei and meiosis to ensure plant viability and fertility. *Frontiers in Plant Science* **10**: 774.

## Supporting Information

Additional Supporting Information may be found online in the Supporting Information section at the end of the article.

**Fig. S1** *In silico* analysis of *Arabidopsis* CAP-D2 and CAP-D3 expression.

**Fig. S2** Protein–protein interaction network of *Arabidopsis* CAP-D2 (condensin I) and CAP-D3 (condensin II).

**Fig. S3** Affinity purification of *Arabidopsis* CAP-D2 and CAP-D3 GS-tagged.

**Fig. S4** Centromeric associations in *Arabidopsis* *cap-d3* mutant and wild-type nuclei.

**Fig. S5** Centromeric areas in *Arabidopsis* *cap-d3* mutant and wild-type nuclei.

**Fig. S6** Nuclear areas of *Arabidopsis* *cap-d3* mutant and wild-type.

**Fig. S7** Immunolocalization of histone modifications in *Arabidopsis* *cap-d3* mutants and wild-type plants.

**Fig. S8** *Arabidopsis* CAP-D2 and CAP-D3 transcription.

**Table S1** Primer sequences and usage.

**Table S2** Antibodies and their dilutions used for immunolocalization.

**Table S3** List of proteins co-purified with CAP-D2-GS.

**Table S4** List of proteins co-purified with CAP-D3-GS.

**Table S5** Differentially expressed genes (DEGs) in the *cap-d3* mutants.

**Video S1** Rotating *Arabidopsis* wild-type nucleus showing ten centromeric signals.

**Video S2** Rotating *Arabidopsis* *cap-d3* *SAIL* nucleus showing three centromeric signals.

**Video S3** Rotating *Arabidopsis* *cap-d3* *SALK* nucleus showing two centromeric signals.

Please note: Wiley Blackwell are not responsible for the content or functionality of any Supporting Information supplied by the authors. Any queries (other than missing material) should be directed to the *New Phytologist* Central Office.